



---

Theses and Dissertations

---

2012-12-07

## Monitoring Land-Cover Change in the Las Vegas Valley: A Study of Five Change Detection Methods in an Urban Environment

Bonnie Diane Weidemann  
Brigham Young University - Provo

Follow this and additional works at: <https://scholarsarchive.byu.edu/etd>



Part of the [Geography Commons](#)

---

### BYU ScholarsArchive Citation

Weidemann, Bonnie Diane, "Monitoring Land-Cover Change in the Las Vegas Valley: A Study of Five Change Detection Methods in an Urban Environment" (2012). *Theses and Dissertations*. 3539.  
<https://scholarsarchive.byu.edu/etd/3539>

This Thesis is brought to you for free and open access by BYU ScholarsArchive. It has been accepted for inclusion in Theses and Dissertations by an authorized administrator of BYU ScholarsArchive. For more information, please contact [scholarsarchive@byu.edu](mailto:scholarsarchive@byu.edu), [ellen\\_amatangelo@byu.edu](mailto:ellen_amatangelo@byu.edu).

Monitoring Land-Cover Change in the Las Vegas Valley: A Study of Five Change  
Detection Methods in an Urban Environment

Bonnie D. Weidemann

A thesis submitted to the faculty of  
Brigham Young University  
in partial fulfillment of the requirements for the degree of

Master of Science

Perry J. Hardin, Chair  
Mark W. Jackson  
Ryan R. Jensen

Department of Geography

Brigham Young University

December 2012

Copyright © 2012 Bonnie D. Weidemann

All Rights Reserved

## ABSTRACT

### Monitoring Land-Cover Change in the Las Vegas Valley: A Study of Five Change Detection Methods in an Urban Environment

Bonnie D. Weidemann  
Department of Geography, BYU  
Master of Science

Change detection is currently a topic of great interest to theoretic geographic researchers. The necessity to map, monitor, and model land cover change is also important to a variety of applied fields as varied as urban planning and military intelligence. This research compares five algorithms to map urban land cover change in the greater Las Vegas, Nevada metropolitan area. Landsat Thematic Mapper imagery acquired on May 1990 and May 2000 was used as the primary data. The change detection methods yielded simple maps of change vs. no change. These algorithms included image differencing, image ratioing, image regression, vegetation index differencing, and principal components analysis. Each of these techniques accurately identified areas of land cover with moderate levels of accuracy and produced overall change detection accuracy values between 60% and 76% depending on the method. The highest accuracy was obtained by the image ratioing method using the red spectral band (76%).

As expected, the determination of change detection thresholds for each technique was critical to the accuracy produced by the algorithm. Moreover, the type of statistic used in optimizing that threshold was also a significant impacting the final accuracy. The approach of using a set of ground points to calibrate the change detection threshold proved to have significant merit.

Keywords: change detection, Las Vegas, threshold, Landsat TM

## ACKNOWLEDGEMENTS

This thesis would not have been possible without the support of many people; most especially by my mentor and dear friend, Dr. Perry Hardin. I express my sincerest gratitude for his exceptional instruction, guidance, advice and encouragement that enlarged my understanding and capabilities throughout my graduate study. I extend special thanks to my committee members Dr. Mark Jackson and Dr. Ryan Jensen for finding time in their busy schedules to support and serve on my committee. Deepest gratitude is also due to Laurie Weisler without whose constant encouragement and assistance this study would not have been successful.

I would also like to express profound love, admiration, and gratitude to my beloved husband and daughter for their patience, understanding, and endless love through the duration of this research. Additionally, I would like to express heartfelt appreciation to my parents for instilling a drive for education and the confidence that I could achieve anything if I set my mind to it.

## Table of Contents

Title Page.....	i
Abstract.....	ii
Acknowledgements.....	iii
Table of Contents.....	iv
List of Tables.....	vi
List of Figures.....	vii
Chapter 1: Introduction.....	1
1.1 Urban Sprawl.....	3
1.2 Monitoring Urban Growth with Satellite Remote Sensing.....	5
1.3 Research Hypothesis and Objectives.....	7
1.4 Significance.....	8
1.5 Structure of Thesis.....	9
Chapter 2: Literature Review.....	10
2.1 Change Detection Methodologies in Remote Sensing.....	10
2.2 Change Detection Methodologies in Urban Environments.....	11
2.3 Image Pre-processing: Preparing Imagery for the Change Detection Process.....	13
2.4 A Review of Common Change Detection Methods.....	14
2.4.1 Algebra.....	16
2.4.1.1 Image Differencing.....	17
2.4.1.2 Image Ratioing.....	18
2.4.1.3 Image Regression.....	22
2.4.1.4 Vegetation Index Differencing.....	23

2.4.2 Transformation.....	25
2.4.2.1 Principal Components Analysis.....	25
2.4.3 Summary of Literature and Conclusion.....	26
Chapter 3: Data, Methods, and Results.....	28
3.1 Study Area.....	28
3.2 Data.....	29
3.3 Image Pre-processing.....	32
3.4 Validation Data: Ground Truth.....	32
3.5 Implementation of Change Detection Methodologies.....	34
3.5.1 Image Differencing.....	34
3.5.2 Image Ratioing.....	40
3.5.3 Image Regression.....	47
3.5.4 Vegetation Index Differencing.....	60
3.5.5 Principal Components Analysis.....	69
3.6 Discussion of Results.....	76
Chapter 4: Discussion and Conclusion.....	77
4.1 Objective 2: Comparing the Methods.....	77
4.2 Objective 3: Threshold Specification.....	81
4.3 Summary.....	82
References.....	85

## List of Tables

Table 1: Summary of Common Change Detection Techniques.....	20
Table 2: Summary of Statistics by Change Detection Technique.....	84

## List of Figures

Figure 3.1 The Greater Las Vegas Metropolitan Area.....	30
Figure 3.2 Landsat TM Image Data.....	30
Figure 3.3 Las Vegas, Nevada Study Area.....	31
Figure 3.4 1990 Reference Image.....	34
Figure 3.5 2000 Reference Image.....	35
Figure 3.6 Image Differencing: Setting a Threshold.....	37
Figure 3.7 Image Differencing: % Accuracy and Threshold.....	38
Figure 3.8 Image Differencing: Chi-Square Statistic and Threshold.....	38
Figure 3.9 Image Differencing Results.....	39
Figure 3.10 Image Differencing: False Color Composite.....	39
Figure 3.11 Image Differencing: Three Band Composite Image: Agree/Disagree Map...40	
Figure 3.12 Image Ratioing: Original, Non-normal Distribution by Band.....	41
Figure 3.12 Image Ratioing: Arc tan Transformation Histograms by Band.....	42
Figure 3.14 Image Ratio Correlation Matrix Using the Absolute Value of the Arctangent Transformation by Band.....	43
Figure 3.15 Image Ratioing: % Accuracy and Threshold.....	43
Figure 3.16 Image Ratioing: Chi-square Statistic and Threshold.....	43
Figure 3.17 Image Ratioing Results.....	43
Figure 3.18 Image Ratioing: False Color Composite.....	46
Figure 3.19 Image Ratioing: Three Band Composite Image: Agree/Disagree Map.....	47
Figure 3.20 Regression Equations by Band.....	48
Figure 3.21 Regression Line for the Green Band.....	48
Figure 3.22 Regression Line for the Red Band.....	49

Figure 3.23 Regression Line for the NIR Band.....	49
Figure 3.24 Image Regression: Residual Images by Band.....	50
Figure 3.25 Image Regression: Histograms of the Residuals by Band.....	52
Figure 3.26 Image Regression: Histogram of the Absolute Value of the Residuals for the Red Band.....	53
Figure 3.27 Image Regression: The Absolute Value of the Residuals for the Green Band.....	54
Figure 3.28 Image Regression: The Absolute Value of the Residuals for the Red Band.....	55
Figure 3.29 Image Regression: The Absolute Value of the Residuals for the NIR Band.....	56
Figure 3.30 Image Regression: Descriptive Statistics by Band.....	56
Figure 3.31 Image Regression: % Accuracy and Threshold.....	57
Figure 3.32 Image Regression: Chi-square Statistic and Threshold.....	58
Figure 3.33 Image Regression Results.....	58
Figure 3.34 Image Regression: False Color Composite.....	59
Figure 3.35 Image Regression: Three Band Composite Image: Agree/Disagree Map.....	60
Figure 3.36 NDVI Values for 1990.....	61
Figure 3.37 NDVI Values for 2000.....	62
Figure 3.38 NDVI Difference.....	63
Figure 3.39 NDVI Absolute Difference .....	64
Figure 3.40 NDVI Absolute Difference Histogram.....	65
Figure 3.41 Descriptive Statistics of Absolute Difference in NDVI since 1990.....	65
Figure 3.42 Figure 3.42 Vegetation Index Differencing: “Best Change” Map.....	66
Figure 3.43 Vegetation Index Differencing: % Accuracy and Threshold.....	67

Figure 3.44 Vegetation Index Differencing: Setting a Threshold.....	68
Figure 3.45 Vegetation Index Differencing: “Best Change” Map Using Chi-square Statistic.....	68
Figure 3.46 PCA: Component Histograms.....	69
Figure 3.47 Setting Two Thresholds for PCA Layers.....	71
Figure 3.48 PCA: Absolute Value Histograms by Component.....	72
Figure 3.49 PCA: % Accuracy and Threshold.....	73
Figure 3.50 PCA: Chi-square Statistic and Threshold.....	74
Figure 3.51 Principal Components Analysis Results.....	74
Figure 3.52 PCA Second Component Change Map.....	75
Figure 3.53 PCA Sixth Component Change Map.....	76

## Chapter 1: Introduction

In 2008, Ban Ki-moon, Secretary-General of the United Nations wrote, “With more than half of the world’s population now living in urban areas, this is the urban century. Harmonious urbanization... has never been more important” (UN-HABITAT, 2008, pg iii). As Ban Ki-moon observed, cities and towns now form the primary habitat for humanity, and improving their livability is vital.

The change from a rural to urban majority has not been temporally or geographically uniform throughout the world. Countries in Latin America, North America and Europe achieved urban majorities in the 1950s and 1960s, whereas nations in Africa and Asia will obtain an urban majority circa 2050. High urban growth rates are primarily phenomena of nations that are transitioning to industrialization; 53% of developing world cities are experiencing an annual growth rate between 2% and 4%. United Nations data from 2007 shows there were 19 cities on the globe with populations exceeding 10 million. By 2025, this list will grow to 26 cities with all the additional members located in Africa and Asia. In contrast, 40% of the cities in developed nations experienced a population *loss* between 1990 and 2000 (UN-HABITAT, 2008). While much of the increase in city population is due to natural increase, complex forces both “push” migrants from rural areas and “pull” them to cities. Push factors include land ownership conflicts, militant insurgency, government land grabs, crop failure, and population pressure. The primary attractant of cities is the perception of economic opportunity along with increased social services. Royuela *et al.* (2010) claims that urban areas exist because cities are the most economically efficient structure to distribute relationships among individuals.

The problems associated with urbanization form a well-known litany. Negative aspects of unmanaged urban growth include air pollution, traffic congestion, increased adolescent crime activity, poor or nonexistent housing for many, disease diffusion, loss of cultural/family identity, and inadequate green space for recreation (Royuela *et al.*, 2010 and deHollander and Staatsen, 2003). These are not just problems of developing countries, but difficulties associated with rapid urban growth in transitional and developed nations too. Given both the positive and negative aspects of urban life, it is critical to study the urban environment and its associated biophysical and social characteristics - especially the quality of human life in urban areas and geographical aspects impacting this urban quality of life.

As the paragraphs above demonstrate, urban growth will be one of the central phenomena of the twenty-first century affecting humanity's well being. Given the need to map, monitor, and measure this change, there is a corresponding need for technological solutions to do this rapidly over large areas using comparable methodologies. This thesis examines the potential to map urban change between two dates using simple change detection techniques performed on satellite imagery. Our primary interest is in detecting change at the periphery of existing urban centers. These periurban zones are areas experiencing poorly managed rapid growth, i.e. urban sprawl. Although the greatest potential for urban/periurban change detection methodology exists in world areas with developing economies, this thesis will present results from experiments conducted in the United States. This was a deliberate choice; for if these methods do not work in the United States where validation and calibration data are widespread and accurate, they

would likely not succeed in areas where such data is sparse and questionable. As such, the United States test case presented in this thesis represents a best-case scenario.

### (1.1) Urban Sprawl

New construction during booming economic times in the US has always lent itself to the concept that more and more people, in pursuit of economic prospects and improved quality of life, contributed to growth in urban areas. Location, or the geography of opportunity, became a factor to determine virtually any aspect of the good life and people's access to it in metropolitan America (Squires and Kubrin, 2005). In 2003 America, urban growth and sprawl were almost synonymous and edge cities became the dominant urban form (Glaeser and Kahn, 2003). As implied above, urban sprawl is the uncontrolled or unplanned extension of urban areas and defined as a dispersed, auto-dependent development outside compact urban centers (Vermont Forum on Urban Sprawl, 2003). Sprawl is typified by low-density settlement, often in erratic building patterns, located along highways in formerly rural areas, and consuming excessive amounts of land (Clarke, 2006).

Like many controversial topics, urban sprawl has triggered an ongoing heated debate and continues to influence legislation. Since the economic downturn as a result of subprime underwriting and predatory lending in the first decade of the 21<sup>st</sup> century, many neighborhoods once booming with prosperity and urban development evolved into foreclosure ghost towns. Half of the United States has enacted laws against predatory lending, reducing the ability for homebuyers and developers to purchase homes and land they would have qualified for previously. In addition, many states, driven by negative factors resulting from urban sprawl, have adopted comprehensive growth management

legislation in an effort to regulate land development more directly (Howell-Moroney, 2007).

Besides its effects on policy, urban sprawl has negatively impacted land and natural resources, infrastructure, real estate development costs, travel and congestion, social policy, and quality-of-life (Burchell *et al.*, 2005). Other activists suggest that the outward expansion of metropolitan areas, particularly given the automobile-dependent lifestyle it nurtures, increases air pollution and a range of diseases including asthma, lung cancer, and heart problems (Squires, 2002).

Despite its negative effects, many researchers view this trend towards increasing urbanization positively, stating the negative quality-of-life impacts are overstated and that effective vehicle pollution regulation has mitigated emission increases associated with increased driving (Glaeser and Kahn, 2003). Consumers apparently agree. In 1999, the National Association of Homebuilders asked two thousand randomly selected households to choose between a large single-family home in the suburbs with a longer commute and a townhouse in the city close to transportation, shopping, and work. Eighty-three percent of respondents chose the larger, suburban or periurban home. This preference for suburbia has dominated development throughout the United States because it provides residents with benefits they value (Burchell *et al.*, 2005).

Regardless of the controversy, many studies agree that urban areas grew significantly over the last fifty years, though both sides disagree over how to measure and interpret its significance (Clarke, 2006). Undoubtedly, the need for such information is valuable as the geography of urban growth offers a graphic depiction of the interplay between economics, political systems, and the environment (Masek *et al.*, 2000). As

human and natural forces modify the landscape, government agencies struggle to monitor and assess these alterations. Changes in vegetation affect wildlife habitats, fire conditions, aesthetic and historical values and ambient air quality that, in turn, influence management and policy decisions (Levien *et al.*, 1998). Changes to the urban landscape due to prolonged protests, civil unrest, and even war can also dramatically affect the distribution of critical necessities to life (e.g. water, food, sanitation, etc.) and the import/export of vital resources. Near real-time information that can provide answers to the dynamic processes within urban and periurban regions is of immense value to planners and administrators (Ahmedabad *et al.*, 1997) as well as heads of state, emergency response officials, and military operations.

#### (1.2) Monitoring Urban Growth with Satellite Remote Sensing

As a result of the unprecedented global shift towards urbanization, a variety of methods have been used to detect, track, measure, and assess urban change. Imhoff *et al.* (1997) stated that the use of satellite remote sensing is an obvious corroborative methodology for measuring and monitoring the location and extent of urbanization and city growth.

Remote sensing is defined as a method used to acquire information about the earth, usually from aircraft or satellites. The information usually acquired on-board the satellite is digital imagery which is subsequently transmitted to earth where analysts use a variety of statistical methods to convert the imagery into informational products such as maps and reports. Satellite remote sensing provides globally consistent, repetitive measurements of the earth's surface relevant to land cover monitoring (Masek *et al.*, 2000) and delivers timely, cost-effective information that conventional methods of urban

data acquisition and survey (e.g. census data, aerial photography) simply cannot provide. In addition to time and cost efficiency, remote sensing is a unique view of the spatial and temporal dynamics in urban growth and land use change (Herold *et al.*, 2003 and Xiao *et al.*, 2006).

Because of these advantages, satellite remote sensing techniques have been widely used in detecting and monitoring land cover change at various scales (Xiao *et al.*, 2006). Stated more formally, change detection methodologies are used to identify differences in the state of an object or phenomenon on successive images observed at different times and can be applied widely to examine changes in the environment (Singh, 1989 and Lu *et al.*, 2004). Many of these change detection methods exist, but no single method is a standard for all research applications. It is a maxim in remote sensing that every target is different, and analyzing it requires both elements of art and science. The maxim holds for change detection. Each change detection project is unique and must cope with peculiar attributes that are original to target, project specifications, or image availability. When faced with a specific scenario where change detection is required, the selection of an appropriate methodology has considerable impact on the accuracy and usability of the final detection product (Lu *et al.*, 2004). Because different change detection algorithms produce different results, experiments where several methods can be applied *to the same area* and compared may be a useful starting point to examine relative strengths and weaknesses of each method. While such experiments would not be able to answer the question of which approach is universally optimal, they may be able to illuminate the relative drawbacks and advantages of each approach over a constant target. In addition, using multiple change detection methods over one study may provide a

measure of guidance for future researchers performing change detection over similar targets. This potential has limits. For example, change detection methods successful for Chicago, Illinois may also prove successful for St. Louis, Missouri or Detroit, Michigan but may fail if applied to San Antonio, Texas or Reno, Nevada because of their different geographic contexts.

### (1.3) Research Hypothesis and Objectives

This research was designed to use satellite remote sensing technology in combination with a variety of change detection methods to detect, measure, and map urban change of the greater Las Vegas area between 1990 and 2000. Imagery from the Landsat Thematic Mapper (TM) sensor acquired in those two years would be used as data. It began with the research question, “What are the relative benefits and drawbacks of each change detection method?” We hypothesized that while all of the methods tested would detect the majority of urban change within the study area, each method would suffer from the problem of “change threshold specification.” This meant that each method would require that an arbitrary decision be made by the practitioner as to what amount of change (as numerically measured by the method) constituted genuine and practically significant change on the ground. This problem is akin to the difficulties experienced by statistical researchers who are faced with the necessity of choosing a level of alpha to either accept or reject a null hypothesis in a social science context. In some situations, choosing one or another of the usual alpha values (e.g. 0.05, 0.01, and 0.005) generates different conclusions vis-à-vis reject or accept the null.

With the research question and hypothesis in-mind, this thesis addresses the following objectives:

- To assess urban change in Las Vegas between 1990 and 2000 using five change detection methods popular in satellite remote sensing.
- To compare the results of the five change detection methods by first, determining the success of the method in capturing change between 1990 and 2000 and second, determining how well each method performed relative to each other.
- To address the problem of change threshold specification by introducing a simple computer method whereby that specification can be done objectively.

This research constitutes a study of methodology, not a study of urban change itself. Thus, while meeting the objectives necessitates some discussion of different land cover types in Las Vegas, it is not intended as an exhaustive discussion on land cover change in Las Vegas per-se, i.e. its historical causes, geographical patterns, and contemporary consequences. In other words, this thesis represents a discussion of change detection methodology in an urban setting using Las Vegas as the study site, but does not represent itself as a historical study of Las Vegas between the year 1990 and 2000.

#### (1.4) Significance

In addition to the savings in resources and time, the study of urban change detection in an arid environment and its methodologies provides a detailed foundation for urban planners and policy makers to make educated decisions that may impact natural resources, surrounding environments and natural habitats, quality of life, and infrastructure needs for communities.

Beyond these necessary and vital applications of change detection methodology domestically is the impact that such research could have for US policy in support of the war fighter abroad. Since 9/11 the United States has engaged in the War on Terrorism

that has taken this country's war fighters to two separate fronts: the Afghanistan/Pakistan border and Iraq. More recently, the Arab Spring has caused a US presence in Libya with potential for boots on the ground in Syria and Yemen. The study of change detection methodologies in this thesis is unique in that the results focus on a study area in the desert regions of the greater Las Vegas area. Similarly, the various fronts engaged in by the United States possess similar physical geographies sensitive to terrorist operations, training, and planning as well as state governments attuned to their objectives. The application of the change detection methods used in this thesis are beneficial to those studying the movement, development, and patterns of terrorists and other independent entities in regions with similar geography and may provide answers and direction for future applications to support the war fighter and intelligence community alike.

#### (1.5) Structure of Thesis

This thesis will proceed in the following manner. Chapter 2 presents a general review of literature detailing change detection studies and methods used to measure and evaluate land cover change using satellite remote sensing. Chapter 3 describes data, methodologies, and results of this study. Finally, Chapter 4 provides a discussion and conclusion with possible directions for future research.

## Chapter 2: Literature Review

### (2.1) Change Detection Methodologies in Remote Sensing

In recent decades the role of satellite remote sensing has expanded at an accelerating rate as human populations grow and occupy ever-increasing space on the earth's surface (Ridd and Hipple, 2006). Though changes to the earth's surface are caused by both anthropogenic and natural factors, the human digital footprint and influence on the earth as captured by satellite remote sensing is detectable, quantifiable, and worthy of examination. As mentioned in the previous chapter, satellite remote sensing is the science of obtaining information about the earth's surface features in a raster image format on a periodic basis from spaceborne or airborne instruments. As such, it provides a means for the mapping, monitoring, and modeling dynamic elements of Earth's surface at regular intervals (Srvastava, 1990). Acquisition of such information via satellites also provides spatially consistent data sets that cover large areas with spatial detail and temporal frequency (Xiao *et al.*, 2006). Example sensors providing this cost-effective multi-spectral and multi-temporal data include the Advanced Spaceborne Thermal Emission and Reflection Radiometer (ASTER), Advanced Very High Resolution Radiometer (AVHRR), Moderate Resolution Imaging Spectroradiometer (MODIS), Satellite Probatoire d'Observation de la Terre (SPOT), Thematic Mapper (TM) and RadarSat. All of these sensors have become a common data source for comparative studies at both temporal and spatial scales (Yu and Ng, 2006).

Thus, satellite remote sensing, as a widespread and effective data source, lends itself to a variety of change detection applications, studies, and methods. Singh (1989) defined change detection as the process of identifying differences in the state of an object

or phenomenon by observing it at different times. Change detection of the earth's surface using satellite remote sensing has been used to examine several dynamic phenomena:

- Natural forest ecosystems (e.g. Coppin and Bauer 1996)
- General landscape change (e.g. Yu and Ng 2006)
- Coastline shifts for environmental management (e.g. Li and Damen 2010)
- Wetland protection and development (e.g. Klemas 2011)
- Land use and land cover change detection of wildlife habitat (e.g. Rahdary *et al.* 2008)
- Environmental degradation processes due to war (e.g. Jabbar and Zhou 2011),
- The growth of urban sprawl (e.g. Davis and Schaub 2005).

## (2.2) Change Detection Methodologies in Urban Environments

Because of its interactions with climate, ecosystem processes, biogeochemical cycles, biodiversity, and human activities, one of the most common applications of remote sensing has been land use/land cover (LULC) change detection (Xiao *et al.*, 2006). Land use can be defined as how the human population utilizes the earth, such as agriculture or urban development. In comparison, land cover is the actual physical material found at the earth's surface, such as conifer, water, asphalt, savanna, etc. The categories of land cover vary from map to map depending on what an analyst is examining. NASA's Earth Observatory (2012) has stated that the only requirement for any land cover category is that it has a distinct spectral signature that a satellite can record. Essentially, LULC change detection is used to determine the type, amount, and location of any LULC difference that has occurred within a specific timespan (Yeh, 1997). Urban sprawl mapping, monitoring, and modeling are the usual goals of LULC

change detection projects in an urban setting (Ahmedabad *et al.*, 1997). With repetitive synoptic viewing capabilities, efficiency and economical value, satellite remote sensing is a powerful tool to detect and map emerging changes in the urban core and peripheral areas of any urban entity (Ahmedabad *et al.*, 1997). Mapping change in the peripheral areas is particularly important. Depending on the global location, these are the areas where important agricultural land may be destroyed, where a societal underclass may create temporary slum housing, where important water resources may be fouled, where sensitive species may be encountered, where land ownership may be poorly documented, or where building and development may be poorly regulated.

Despite the number of studies of urban change detection analysis, a consensus regarding the best methodology has not emerged (Almutairi and Warner, 2010). This is due in part to the nature of the urban target itself. In highly urbanized areas, identifying the extent of urban sprawl can be challenging. The number of mixed signature pixels increases as the land cover types increase, and is inversely related to spatial resolution.

This complex process is characterized by the presence of numerous surface materials in relatively small regions. The features in these urban scenes contribute to the reflected radiance and are difficult to detect by coarse sensors. Urban areas are typified by intricate mixture of materials ranging from concrete, wood, tiles, bitumen, metal, sand, and stone. The spatial distribution of these materials is not regular and is compounded by rapid temporal changes that occur in the urban landscape over a very short period of time (Bhaskaran and Datt, 2000).

As spatial resolution affects the heterogeneity of land cover classes in studies of densely suburban metropolitan regions, small problems can become magnified: trees on lawns are confused with forest classes; grassy areas are common in pasture, recreation, and institutional classes; and pavement is common to both high-density residential and

commercial/industrial areas (Epstein *et al.*, 2002). Due to the complexity of urban areas and the variety of classes within each pixel, uncertainty between classes that contain similar components is frequent. This further complicates the process to find an effective change detection method for urban applications. However, Lu *et al.* (2004) stated that different change detection algorithms have their own merits and that no single approach is optimal or applicable to all cases. Therefore in practice, an analyst should select several methods to implement change detection in a study area and then compare and identify the best results through accuracy assessment (Lu *et al.*, 2004). Because experimentation is warranted, knowledge of common and effective change detection methods is needed by the change detection researcher.

### (2.3) Image Pre-processing: Preparing Imagery for the Change Detection Process

Prior to applying a change detection algorithm, appropriate pre-processing of the remote sensor data is required. Only imagery that has been accurately georegistered, normalized, and subset into processing areas can be submitted to the change detection process (Levien *et al.*, 1998). To speak more precisely, the following conditions must be satisfied: (1) precise registration of multi-temporal images; (2) precise radiometric and atmospheric calibration or normalization between multi-temporal images; (3) similar phenological states between multi-temporal images; and (4) selection of the same spatial and spectral resolution images if possible (Lu *et al.*, 2004).

The first condition is more commonly called geometric correction or spatial registration. This step is crucial to the success of a change detection algorithm because it ensures that a pixel at one date overlaps the identical pixel on the second date (Townsend *et al.*, 1992 and Macleod and Congalton, 1998). Poor spatial registration can cause errors

in the final results. For example, a misregistration of just one pixel may cause a stable road on the two dates to show up as a new road in the change image (Jensen, 2005).

The result of the second condition, radiometric calibration, is that units become constant between images. Calculation of radiance is the fundamental step in putting data from multiple sensors and platforms onto a common radiometric scale (Chander *et al.*, 2007). Additionally, removing any effects of the atmosphere from the imagery allows for the interpretation of the image data to be consistent and continuous.

The third and fourth conditions to be met prior to the application of any change detection method are the selection of similar phenological states between multi-temporal images and the selection of the imagery with the same spatial and spectral resolution, respectively. Obtaining near-anniversary images greatly minimizes the effects of seasonal phenological differences that may cause spurious change to be detected in the imagery (Jensen, 2005). Additionally, the assumptions behind the change detection processes are challenged when the spectral range of a band from one sensor system does not match that of another system. In such a case the analyst is left hopelessly comparing apples to oranges. Moreover, selecting imagery from different dates with different spatial resolution may not just harm the change detection result, but will cause for significant pre-processing headaches to ensure both images are truly comparable.

#### (2.4) A Review of Common Change Detection Methods

Various digital algorithms have been developed for change detection in remote sensing. Some have grown in popularity, whereas others are peripheral to the mainstream of topic. Combining observations by Singh (1989) and Liu *et al.* (2004), popular methods include the following:

- Image differencing
- Image ratioing
- Image regression
- Vegetation index differencing
- Principal component analysis (PCA)
- Multi-date classification\*
- Post-classification comparison\*
- Change vector analysis\*
- Background subtraction

Examining these varied techniques remains an active research topic due to the efficacy and efficiency in employing these methods. Even more so, it reflects the unique spatial and spectral attributes of different earth locations that demand different remote sensing approaches. As a result, the literature does not reflect a “go-to” algorithm for change detection applications across the board.

Many of the methodologies listed above have been comprehensively reviewed (Singh 1989, Coppin and Bauer 1996, Liu *et al.* 2004, Lu *et al.* 2004). In this research we will only examine change detection methods yielding change/no-change results. This excludes change detection methods that require land use classification as a prior step. These are marked with an asterisk in the list above.<sup>1</sup> The reason we exclude these methods is to avoid the necessity of discussing and managing the challenges inherent in land cover classification itself (Hardin and Hardin, 2013) which are multiplied when two

---

<sup>1</sup> In making this exclusion, we admit that these land cover-based methods do provide change/no-change information (Jensen, 1981), although this is seldom the sole goal of the researcher using these approaches since much more economical approaches exist.

dates of imagery are examined. This deliberate exclusion effectively limits the scope of the research to a manageable level.

In order to keep the remaining popular change detection methods in their proper theoretical families, they can be grouped into two categories: (1) Algebra and (2) Transformation. For the two categories, family member descriptions, advantages, disadvantages, and supporting literature are provided in Table 1. The majority of the techniques reviewed for change detection utilized data with moderate spatial resolution such as Landsat MSS, TM, or SPOT.

#### (2.4.1) Algebra

The algebra category includes the following methods: image differencing, image ratioing, image regression, and vegetation index differencing. These techniques share two common characteristics. First, they each involve the mathematical combination of imagery from different dates (Mas, 1999). Second, they require the selection of thresholds to determine the changed areas (Lu *et al.*, 2004). This second characteristic is a distinct disadvantage. We admit that selecting suitable image bands and ensuring that critical geographic registration and radiometric normalization can help to limit the problems of threshold determination, but suitable band selection cannot eliminate it.

Threshold selection introduces an obnoxious complication into change detection methodology. It requires that the researcher specify a numerical cutoff value. Image values below the cutoff are designated “no change” whereas image values above the cutoff value are classified as “change.” In our experience, there is no natural cutoff value depicted in a histogram to help the researcher. If the cutoff value is set too high, then bona fide change is not recorded in the final map. If the cutoff value is set too low, then

false positives result, i.e. areas are marked as changed where no substantive change actually occurred.

When selecting which spectral bands to use for each change detection method, most textbooks present the selection as a critical and pressing issue. Use of the infrared or red bands is considered the best practice for most targets. While this may simplify matters, there really is no obvious necessity to select the “best” image band for change detection at all. Instead, a better approach would be to repeat the change detection on several of the available bands and use the individual results as a self- or cross-validation. Alternatively, they could be treated heuristically as three separate judges of change, and a voting strategy might be implemented to make the final decision of altered/not altered from among the several results. We find it puzzling that this approach is not common in the literature.

#### (2.4.1.1) Image Differencing

In this method, registered images acquired at different times are subtracted, pixel by pixel, to produce a residual image composed of the numerical differences between the pairs of pixels (Mas, 1999, and Ridd and Liu, 1998). Mathematically,

$$Dx_{ij}^k = x_{ij}^k(t_2) - x_{ij}^k(t_1)$$

where  $x_{ij}^k$  = the pixel value for band  $k$ , and  $i$  and  $j$  denote the line order and column order of the pixel in this image pair,  $t_1$  = first date and  $t_2$  = second date (Singh, 1989 and Liu *et al.*, 2004). Values in the residual image that equal zero reflect areas of no change, or equal reflectance, in both images. When the results are displayed using common statistical graphics, this technique produces a histogram with a difference distribution for each band. A critical element of the image differencing method is deciding where to

place the threshold boundaries between change and no-change pixels displayed in the histogram (Singh, 1989). While selecting the threshold properly can be difficult, when done correctly, it should help remove differences within the imagery that were present due to variation in bidirectional reflectance and differences due to atmospheric effects (Quarmby and Cushnie, 1989).

According to Singh (1989), image differencing is the most widely used technique for change detection and has been used in a variety of geographical environments. Sunar (1998) applied the image differencing technique to detect land cover changes and development pressures in Istanbul, Turkey. In that study, the researcher found that image differencing to be “relatively straightforward” and did not require significant *a priori* knowledge of the scene and the application. Quarmby and Cushnie (1989) also applied this technique in southeast England to monitor urban land cover changes at the urban fringe. The authors used the technique successfully with the ability to “delineate areas of change in land use from rural to urban development.” However, using TM bands two and four, Mas (1999) found this method to be inferior to other algebraic and post-classification procedures. Nonetheless, in a comparative method study, Lu *et al.* (2004) found this technique to be “simple” and “easy to interpret” as well as suitable for identifying image bands and thresholds.

#### (2.4.1.2) Image Ratioing

This technique is similar to the image differencing method with regards to its straightforward application and disadvantages, though it is not as widely used. Like the image differencing technique, the image ratio method is also a pixel by pixel operation that compares two images by use of a simple mathematical operator (Liu *et al.*, 2004).

The formula is simple;

$$r_{ij} = x_{ij}(t_1) / x_{ij}(t_2) ,$$

where  $r_{ij}$  is the ratioed value (Liu *et al.*, 2004). Values in the quotient image that equal one indicate areas of no change (i.e., equal reflectance on both dates), while change is recorded as values greater than or less than one. In one project, Lu *et al.* (2004) stated that image ratioing reduces the impacts of sun angle, shadow and topography while Prakash and Gupta (1998) stated that the use of image ratio made no marked improvement over other methodologies as applied in a coral mining area in India. Nelson (1983) examined the use of image ratioing to detect gypsy moth defoliation and found that a difference of the MSS7/MSS5 ratio was more useful in the delineation of said areas than any single band-pair ratio. Stow *et al.* (1990) also found that image ratio was a useful land-use change technique and that by ratioing red and near-infrared bands of a

Table 1. Summary of Common Change Detection Techniques

Algorithm	Description	Advantages	Disadvantages	Literature
Category I. Algebra				
Image Difference	Two multi-temporal images are subtracted from one another to create a residual image	Very simple to execute, results were easy to interpret	Must determine thresholds, accurate geometric registration and radiometric normalization is critical, describes change/no change only	Lu <i>et al.</i> (2004), Mas (1999), Quarmby and Cushnie (1989), Singh (1989), Sunar (1998)
Image Ratio	Two multi-temporal images are divided, one by the other.	Straightforward and simple to execute	Must determine thresholds from a possible non-normal distribution, does not provide detailed "from-to" data, describes change/no change only, often criticized for non-normal distribution	Liu <i>et al.</i> (2004), Lu <i>et al.</i> (2004) Nelson (1983), Prakash and Gupta (1998), Robinson (1979), Singh (1989), Stow <i>et al.</i> (1990)
Image Regression	A relationship is established between two multi-temporal images, then pixel values of the second date are estimated using a regression function, then pixel values from the first date are subtracted from the predicted pixel values of the second	Reduces the impact of radiometric heterogeneity (i.e. atmosphere, sensor calibration, Sun angle, etc), also relatively simple to employ	Must determine a regression model to best estimate the the pixel values of the second-date image, must determine thresholds to detect change, yields change/no change results only	Berberoglu and Akin (2009), Liu <i>et al.</i> (2004), Madanian <i>et al.</i> (2012), Ridd and Liu (1998), Theau (2008)

Table 1. Summary of Common Change Detection Techniques

Algorithm	Description	Advantages	Disadvantages	Literature
Category I. Algebra				
Vegetation Index Differencing	The vegetation index is calculated for each image separately, then they are subtracted from one another	Emphasizes differences in the spectral response of various features and reduces impacts of topographic effects	Can overestimate areas of change and gives some indication of inherent noise, selection of thresholds to detect change must also be determined	Mas (1999), Lu <i>et al.</i> (2004), Lunetta <i>et al.</i> (2006), Nelson (1983), Singh (1989), Thanapura <i>et al.</i> (2006), Yuan and Bauer (2006)
Category II. Transformation				
Principal Components Analysis	Two or more multi-temporal images are stacked in a single file and PCA is performed, after which the component images are analyzed for change information	Reduces data redundancy	Requires good knowledge of the study area, difficult to interpret, and selecting thresholds to determine change and no-change areas	Byrne and Crapper (1980), Ceballos <i>et al.</i> (1997), Lu <i>et al.</i> (2004), Singh (1989), Theau (2008), Toll <i>et al.</i> (1980), Yeh (1997)

Landsat MSS–SPOT multi-temporal pair produced about 10% higher change detection accuracy than ratioing similar bands of a Landsat MSS–Landsat TM multi-temporal pair.

As mentioned above, this technique is not as widely used as others. Perhaps it is because this technique can produce a histogram with a non-normal distribution, increasing the challenge in selecting a threshold between change and no change. If the distributions are non-normal and functions of the standard deviations are used to delimit change from no change, the areas delimited on either side of the mode are not equal; therefore, the error rates on either side of the mode are not equal (Singh, 1989). Nevertheless, Robinson (1979) and Singh (1989) recommend that the further studies of the ratioing method under a variety of conditions would be useful.

#### (2.4.1.3) Image Regression

In image regression, the brightness values from one multi-temporal image are assumed to be a linear function of the values of the same area at another time (Liu *et al.*, 2004). This suggests that a majority of the pixels experience no change between the two dates. Given this assumption, this method regresses  $x^k_{ij}(t_1)$  against  $y^k_{ij}(t_2)$  using a regression function that best describes the relationship between pixel values of each spectral band from the two dates. Ordinary least squares is typical, although not mandatory (Berberoglu and Akin 2009, Ridd and Liu 1998, and Liu *et al.* 2004). A simple bivariate linear regression function may be written as:

$$y^k(t_2) = mx^k(t_1) + b,$$

where pixels of band  $k$  from  $t_1$  are represented by the independent  $x$  and the pixels of band  $k$  from  $t_2$  are represented by the dependent  $y$ . Coefficients  $m$  and  $b$  are the slope and intercept, respectively. In change detection, the slope value is usually close to one. The

intercept can vary widely. Both the slope and intercept have interpretations related to atmospheric distortion, sun angle, and other factors. In change detection, the residuals are the primary product of interest. Once the regression between band pairs is run and coefficients are determined, the residuals are then computed using the image difference formula where  $re_{ij}$  is the final transformed value in the residual image and  $y^{k}_{ij}(t_2)$  is the predicted values for the second date.

$$re_{ij} = y^{k}_{ij}(t_2) - x^{k}_{ij}(t_1)$$

The residuals of the regression function are considered to represent the areas of change (Theau, 2008). Like the other methods in the Algebra category, image regression requires the selection of a threshold to determine pixels of change and no change.

According to Berberoglu and Akin (2009) and Theau (2008), this technique reduced the effects of radiometric heterogeneity (i.e. atmospheric conditions, Sun angle, and sensor calibration). In a comparison study, Madanian *et al.* (2012) used image regression, image ratioing, and image differencing to monitor LULC change in Isfahan, Iran. The authors concluded that image regression yielded the least overall accuracy and did not provide detailed information about the kinds of land cover change detected. However, Ridd and Liu (1998) compared image differencing, image regression, the Kauth-Thomas transformation, and the Chi-square transformation for urban land-use detection in the Salt Lake Valley and concluded that image differencing and image regression were the best methods using Landsat TM band 3. However, the authors also stated that none of the algorithms used was overwhelmingly superior to the other.

#### (2.4.1.4) Vegetation Index Differencing

Vegetation indexes are popular in remote sensing, and several exist. See Jensen

(2005) for a complete introduction. Speaking generally, vegetation indexes are used to quantify the amount, health, moisture status, phenological stage, or photosynthetic activity of vegetated surfaces, both natural (e.g. grassland) or anthropogenic (e.g. cropland). Vegetation index differencing is a simple, straightforward technique used to assess whether or not the study target has changed in amount, health, etc. Historical inertia, as well as the positive characteristics of the Normalized Difference Vegetation Index (NDVI) has made it the vegetation index of choice in many applications. As defined by its originator Rouse (1974),

$$NDVI = (NIR - RED) / (NIR + RED)$$

where NIR is the near-infrared band response for a given pixel and RED is the red band response (see also Mas, 1999). This NDVI equation produces values in the range from -1 to 1, where positive values indicate vegetated areas and negative values signify non-vegetated surface features (Yuan and Bauer, 2006). When used in change detection, the vegetation index is first calculated on a pixel-by-pixel basis for both dates separately. Subsequently, the second-date vegetation index is subtracted from the first-date vegetation index (Lu *et al.*, 2004). Like the other methods discussed above, determination of a threshold to highlight areas of change and no change is required. Though this method is typically applied in studies to assess the maturation, health status, expansion or even reduction of vegetation, it is also useful for urban change applications due to its ability to highlight impervious surfaces or a shift from pervious (i.e. vegetated) to impervious (e.g. urban concrete) conditions.

Nelson (1983) tested the method quantitatively in the study of gypsy moth defoliation in Pennsylvania. His results indicated that of the three change detection

methods applied (image differencing, image ratioing, and vegetation index differencing), the latter most accurately delineated forest canopy change. Thanapura *et al.* (2006) used this technique to map impervious area and open space with an overall accuracy of 92%. Moreover, Lu *et al.* (2004) found that vegetation index differencing emphasizes differences in the spectral response of different features and reduces impacts of topographic effects and illumination. Alternatively, Lunetta *et al.* (2006) found some indication of the inherent noise level in a study of land cover change in the Albemarle-Pamlico Estuary System region of the US as well as an overestimation of change area. In another project, Singh (1989) stated it is difficult to draw any firm conclusion about the capability of this technique.

#### (2.4.2) Transformation

For the sake of this research, the transformation category of change detection methods contains the following single approach: principal components analysis (PCA). While other transformations do exist (e.g. Tasseled-Cap transformation), PCA is the most common. Other transformations such as multivariate alteration detection or Gram-Schmidt transformation have also been developed though they are used to a much lesser extent by most practitioners, and are virtually nonexistent in commercial image processing software (Theau, 2008).

##### (2.4.2.1) Principal Components Analysis

Principal components analysis is a type of linear transformation that is often used to reduce spectral data dimensionality by creating fewer new components (Theau, 2008). This technique can be applied in two ways: (1) put two or more dates of images into a single file, then perform PCA and analyze the minor component images for change

information; and (2) perform PCA separately, then subtract the second-date PC image from the corresponding PC image of the first date (Lu *et al.*, 2004). After performing a PCA, unchanged areas are mapped in the first or second component (i.e. information common to multi-date images) whereas areas of changes are mapped in the last components (i.e. information unique to either one of the different states) (Theau, 2008). The assumption for this is that areas of change occupy only a minor proportion of the entire study area and therefore are not reflected in the first two components which explain most of the variation (Yeh, 1997). We note that in change detection PCA is usually performed using the variance-covariance matrix rather than the correlation matrix (Singh, 1989).

In a review of the method, Theau (2008) found the accuracy of change detection via PCA was highly scene dependent and difficult to interpret. Similarly, Stow *et al.* (1990) found that ratioing multi-sensor, multi-temporal satellite image data produced higher change detection accuracy than PCA. Moreover Toll *et al.* (1980) and Singh (1989) reported that principal components transformation used for urban change detection produced lackluster change detection results compared with image differencing of band 2 or 4 (sensor unspecified). However, not all results using PCA have been negative. Byrne and Crapper (1980) monitored land cover changes in Bay, New South Wales using PCA and stated that the method was an effective way to identify areas of change. Additionally, Ceballos and Bottino (1997) discovered that when applying a simple cluster method on two principal components, various types of vegetative landscape could be discriminated with a quality similar to the use of all six bands.

#### (2.4.3) Summary of Literature and Conclusion

A thorough review of the literature does reveal that each of these change/no-change methods for determining change using remote sensing have potential to succeed in multiple environments when caution is exerted towards their challenges and their advantages exploited. The majority of these change detection methods are simple to execute and straightforward in their application and analysis, though each requires attention to the selection of thresholds to accurately determine areas of change/no-change. This is of note when the purpose of the change detection is for a quick, clear result, such as in emergency response, military operations, or national security. As mentioned previously, none of the methods selected for this study will provide a detailed “from-to” explanation of change, but a simple analysis examining change/no-change results. While other research studies do examine multiple change detection methodologies over a study area, such as Lu *et al.* (2004), Mas (1999), or Singh (1989), in my review of the literature, a study of simple change/no change methodologies for the purpose of streamlining the selection process for others in need of quick, accurate techniques does not exist.

This study of five change detection methods of the greater Las Vegas metropolitan area to detect urban growth will attempt to answer the question “What are the relative benefits and drawbacks of each change detection method?” and help narrow the scope for analysts in need of a fast, uncomplicated algorithm to assist them in identifying change in urban settings set in environments with similar physical and geographic characteristics, i.e. urban areas experiencing growth or change in desert climates.

## Chapter 3: Data, Methods, and Results

This thesis had three objectives. The first objective was to assess urban change in a desert study area between 1990 and 2000 using five change detection methods popular in satellite remote sensing. The second objective was to compare the results of the five change detection methods by determining the success of the method in capturing change between 1990 and 2000 and then determining how well each method performed relative to one another. The last objective was to address the issue of change threshold specification by introducing a simple computer method whereby that specification could be done objectively.

### (3.1) Study Area

The Las Vegas valley in southern Nevada encompasses approximately 621.4 mi<sup>2</sup> or 1,609 km<sup>2</sup> and is surrounded by the Spring and Sierra Nevada mountain ranges, with Mount Charleston located to the northwest. The vegetation in the valley is sparse though it can be found more abundantly in the landscaping of urban areas. Even so, native stone and crushed rock are widely used for landscaping as well as gravel, concrete, and other xeriscape methods which employ small amounts of photosynthesizing vegetation (Xian *et al.*, 2008). Located along the 36<sup>th</sup> parallel, the Las Vegas valley is characterized by a desert climate with extremely hot, dry summers and relatively cool, wet winters.

The Las Vegas valley includes the cities of Las Vegas, North Las Vegas, Henderson, and Boulder City within Clark County (see Figure 3.1). According to the Las Vegas government (2012), the city was founded on 15 May 1905 after the population rose due to the completion of a main railway linking Salt Lake City with southern California and with the availability of water, Las Vegas became a major refueling point

and rest stop. With legalized gambling in 1931 and the subsequent completion of the Hoover Dam, the population continued to grow into the following decades. Following WWII, luxurious hotels and casinos began to appear and tourism became the number one employer in the valley (Las Vegas Government, 2012). The region experienced remarkable growth as the population increased from less than 50,000 in Clark County in 1950 to more than 1.37 million in 2000 (Clark County, 2005). As of the 2010 census, the population of the Las Vegas metropolitan area in Clark County stood at 1,951,269, a marked increase of 41.8% since 2000. Associated with the population increase is the growth in residential and commercial development in the area (Xian *et al.*, 2008). Housing units reached approximately 540,000 in 2000 and single-family detached housing and apartments comprised 53.3 percent and 27.6 percent, respectively of total housing units in the urban area (Xian *et al.*, 2008). Such marked changes to a desert landscape in a relatively brief period of time provide for ideal study conditions for the application of change detection methodologies.

### (3.2) Data

Two images for this study were acquired from the U.S. Geologic Survey's Earth Explorer ([www.earthexplorer.usgs.gov](http://www.earthexplorer.usgs.gov)). The images were captured using the Landsat Thematic Mapper (TM) sensor on 16 May 1990 and 11 May 2000 (see Figure 3.2). Consistent with best practices in change detection studies, anniversary dates were employed to reduce potential challenges from sun angle differences and vegetation phenology changes (Singh, 1989). Landsat TM data was selected for this study as this platform was designed and continues to operate with the objective of tracking changes in land cover conditions (Masek *et al.*, 2000). In fact, the Landsat dataset is the only long-



Figure 3.1 The Greater Las Vegas Metropolitan Area (<https://maps.google.com>, 2012)

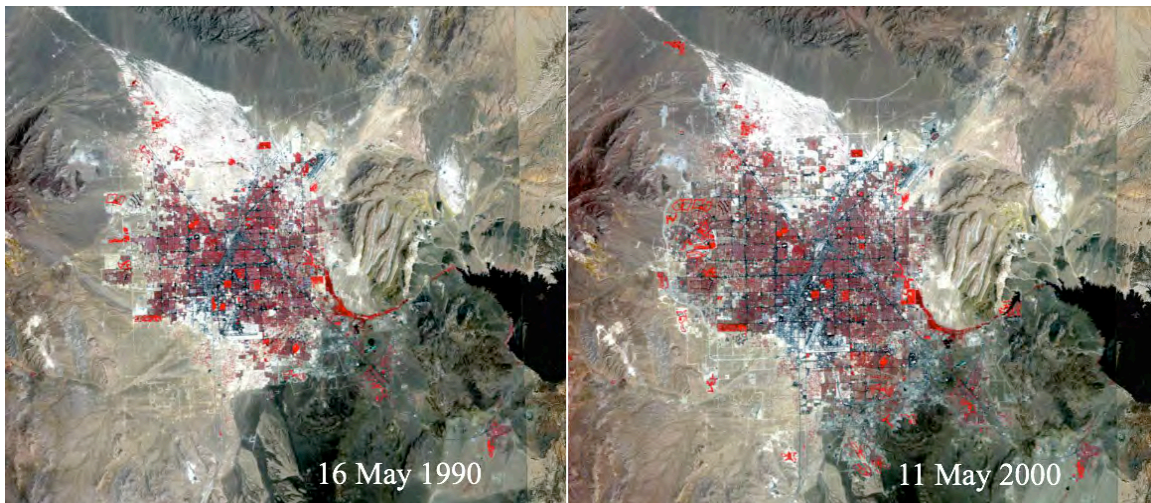


Figure 3.2 Landsat TM Image Data

term digital archive with a medium spatial resolution and relatively consistent spectral and radiometric resolution (Yang *et al.*, 2003). Landsat TM features seven bands of image data, three in the visual spectrum and four in the infrared. All bands possess an instantaneous field of view (IFOV) of 30 x 30 meters with the exception of the thermal infrared band's IFOV of 120 x 120 meters. However, for this study, bands 2, 3, and 4 (i.e. green, red, and near-infrared respectively) were utilized.

For each test site, the regions comprising the cities, suburban development, and urban expansion were subsetting to produce the test data (see Figure 3.3). For the Las Vegas valley this was easy to distinguish and accomplished by visually examining the line between urban and desert. A mask layer was created by hand to exclude all pixels outside the study area. In all the reported statistics, these masked-out pixels are ignored.

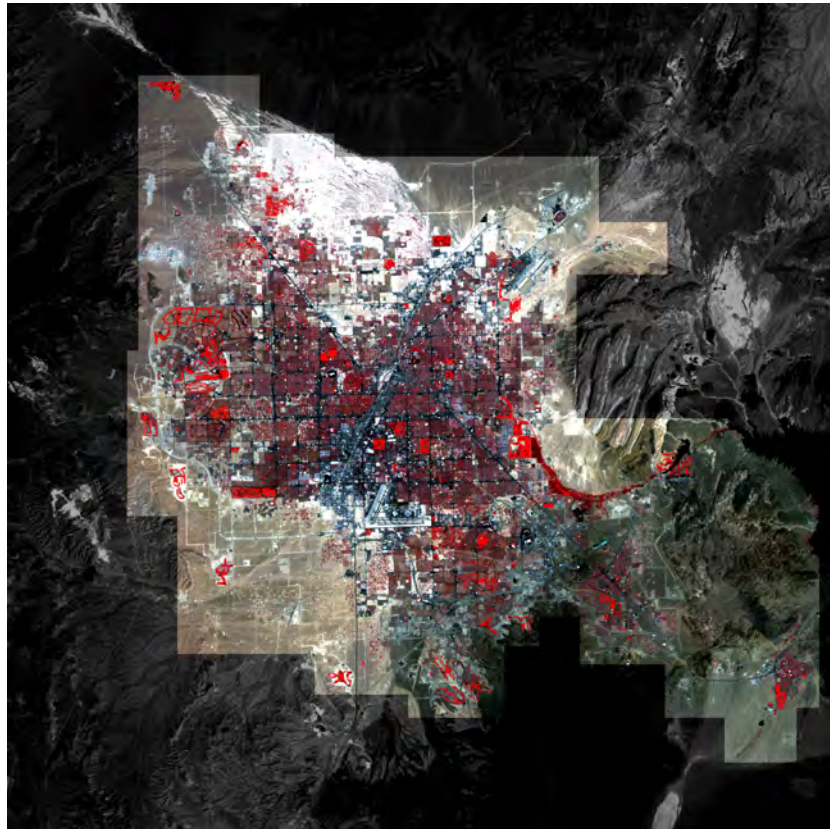


Figure 3.3 Las Vegas, NV study area.

### (3.3) Image Pre-processing

Prior to receiving the study imagery from the USGS Earth Explorer, both images were geometrically registered. Examination of the image metadata revealed that both images were resampled to a Universal Transverse Mercator (UTM) projection and 30 by 30-meter pixels using the cubic convolution transformation technique, with a root mean square error of less than 0.135, or less than 1 pixel. After a side-by-side visual inspection of both images, it was clear that the two datasets coregistered exactly, pixel by pixel. As a result, no further georeferencing methods were required.

Manual radiometric calibration for both images was required to ensure the imagery was set to a common scale. Both Landsat TM images were calibrated to exoatmospheric reflectance ( $r_p$ ) using the following algorithm:

$$r_p = (\pi * L_l * d^2) / (ESUN_l * \cos q_s)$$

where  $L_l$  is the spectral radiance,  $d$  is the Earth-Sun distance in astronomical units,  $ESUN_l$  is the mean solar exoatmospheric irradiance, and  $q_s$  is the solar zenith angle in degrees.

$ESUN_l$  is derived from tables provided in the Landsat Technical Notes (August 1986).

This calibration process was executed by following a help file for Landsat TM

Calibration in the Exelis ENVI geospatial image processing software. The result of radiometric calibration is that units (i.e. percent reflectance) were comparable between the two images.

### (3.4) Validation Data: Ground Truth

In most remote sensing, the gathering of ground truth data is necessary. Ground truth data forms a control for what is being modeled in the imagery. In this research the ground control data was used for both calibration and validation. The calibration ground

control data was used to set the threshold for change / no change using the iterative method described below. The validation set was used to provide an uninflated measure of change detection on a second set of points. The use of separate calibration and validation sets is common in scientific studies that use regression methods, i.e. one set of data is used to determine the coefficients of the regression equation whereas the second set, submitted to the calibrated regression equation, provides an accurate measure of its predictive value.

In this study, 500 points were chosen at random throughout the study area to assess points of actual change. Using images from 1990 and 2000 as references, it was manually recorded for each of these points whether the land cover changed or not. These points were divided into two sets of 250 points each, a set for calibrating the threshold and a cloistered set for assessing the accuracy of the calibrated model.

The images used to generate these sample points are worthy of note. The 1990 reference image was a mosaic of DOQ's (digital orthophoto quadrangles) from 1990 and 1994 (see Figure 3.4) as acquired from the U.S. Geologic Survey's Earth Explorer ([www.earthexplorer.usgs.gov](http://www.earthexplorer.usgs.gov)). Because this mosaic contained images from 1994 but was used as the 1990 reference image, the possibility exists that change during the years of 1990 and 1994 may have been incorrectly marked as no change. As a result, 31% of the 1990 reference points came from the 1990 DOQ, while the remaining 69% came from 1994. Additionally, the original spatial resolution was 1-meter, but the image was resampled up to 7.5-meter spatial resolution for increased ease in comparing the two dates.

Similarly, the 2000 reference image, also acquired from the USGS Earth

Explorer, was captured using the Landsat 7 or Enhanced Thematic Mapper Plus sensor using the pan-sharpened band, i.e. band 8. Spatial resolution of this reference image was 15 meters. Please see Figure 3.5 for reference.

### (3.5) Implementation of Change Detection Methodologies

#### *(3.5.1) Image Differencing*

In this study, the 1990 image was subtracted from the 2000 image. The absolute value of this method was then computed. This step removes the direction (positive or negative) that reflectance changed between the two years yielding the magnitude of

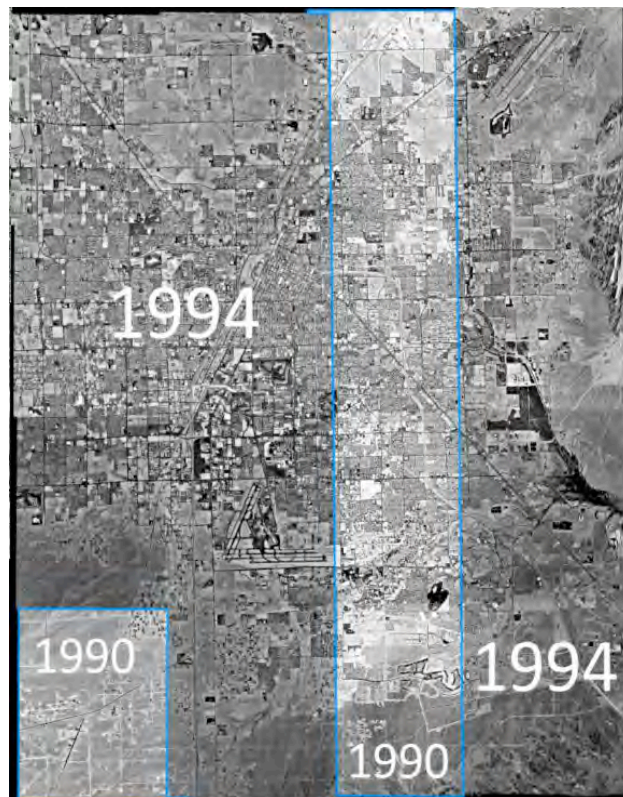


Figure 3.4 1990 Reference Image



Figure 3.5 2000 reference image.

change in reflectance. Thus, values greater than zero indicate magnitude of change in percent reflectance since 1990 and values equal to zero indicate no change in percent reflectance since 1990.

At this point, the change images for the three bands (Green, Red, NIR) had a range of possible values. It was necessary to set some threshold, unique to each band, to determine areas of change and no change (see Figure 3.6). To determine the best threshold, one hundred different thresholds were tested. At each threshold, the chi-square statistic was measured and the percent of calibration points accurately classified were recorded. The chi-square statistic applied is a measure of how good the change map for a single band follows the expected distribution of change based off of the calibration data. The validation data was then submitted to the calibrated system. Two graphs were created to identify patterns. The first graph (see Figure 3.7) plotted the percent of accurately

identified validation data samples (% of accuracy) against the tested thresholds. Please note how regardless of which band, the percent of accurately identified validation data followed the same pattern as the threshold increased. In the second graph (see Figure 3.8) we plotted the chi-squared statistic against the tested thresholds. The graph followed the same trend as the previous graph where, regardless of band, the chi-squared statistic followed the same pattern as the threshold increased. The minimum chi-square statistic for each band and its associated threshold and % accuracy are shown in the table below (see Figure 3.9).

All three change maps were then combined to create a false color composite image (see Figure 3.10). Intersecting the areas of change between the three maps produces areas of agreement (white) and areas of disagreement (colored). Additionally, a map composite image of all three change maps reflecting areas of agreement and disagreement only was also created (see Figure 3.11). Green indicates areas of agreement between the three change maps while blue indicates areas of disagreement. Using the principle of agree and disagree: this false color composite image of all three change maps reveals that all three change maps agree that 11% of the study area changed and disagree whether an additional 8.3% of the study area changed.

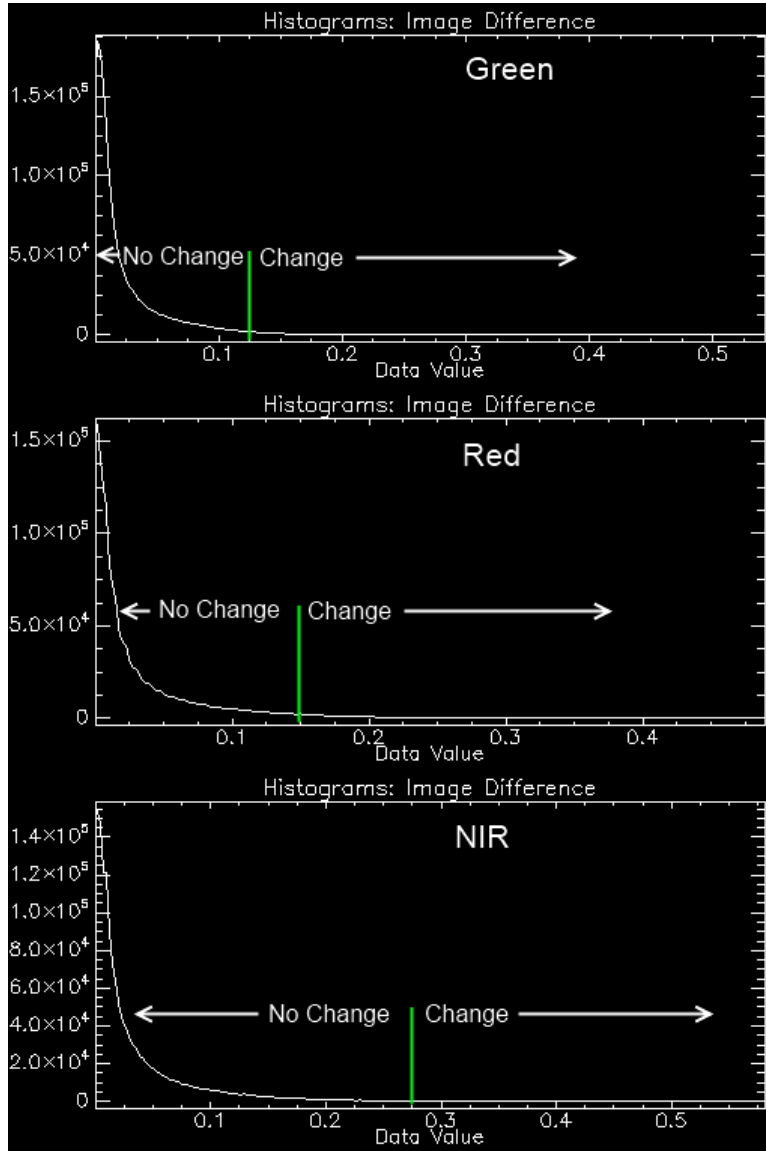


Figure 3.6 Image Differencing: Setting a Threshold

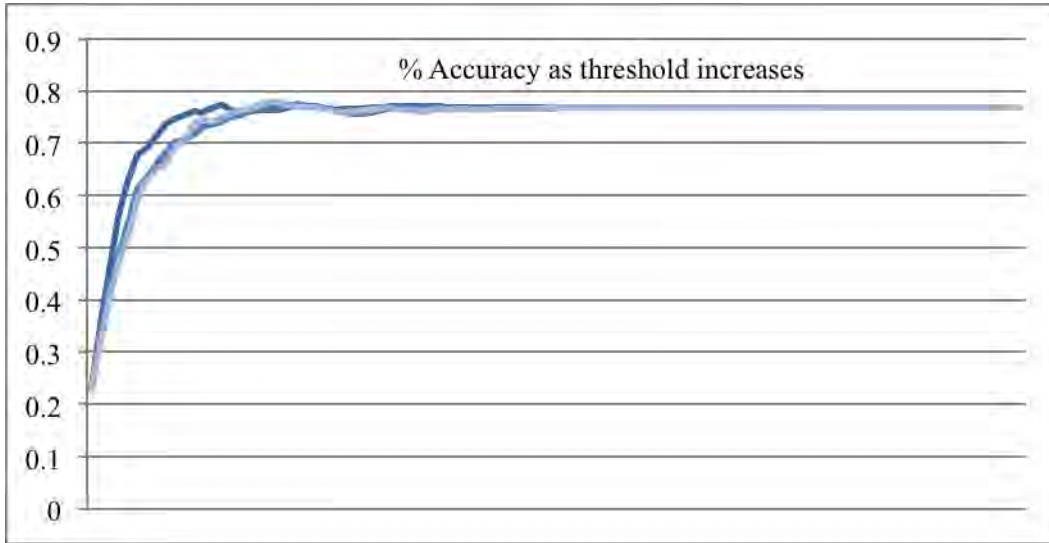


Figure 3.7 Image Differencing: % Accuracy and Threshold

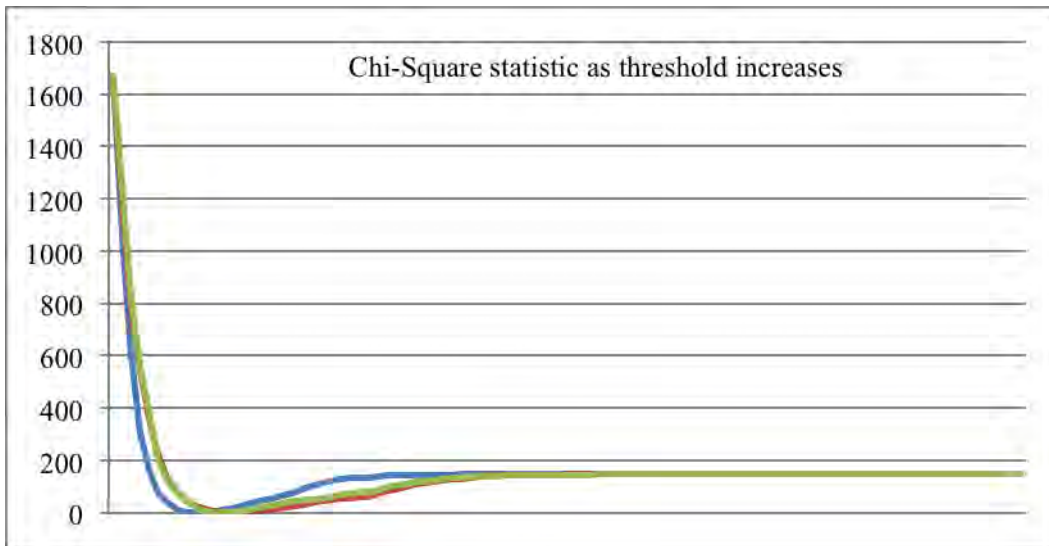


Figure 3.8 Image Differencing: Chi-Square Statistic and Threshold

	Threshold	Accuracy	Min (Chi-Squared)
Green	0.0488	74.8%	0.0452
Red	0.0685	74.2%	0.1016
NIR	0.0697	74.8%	0.1807

Figure 3.9 Image Differencing Results

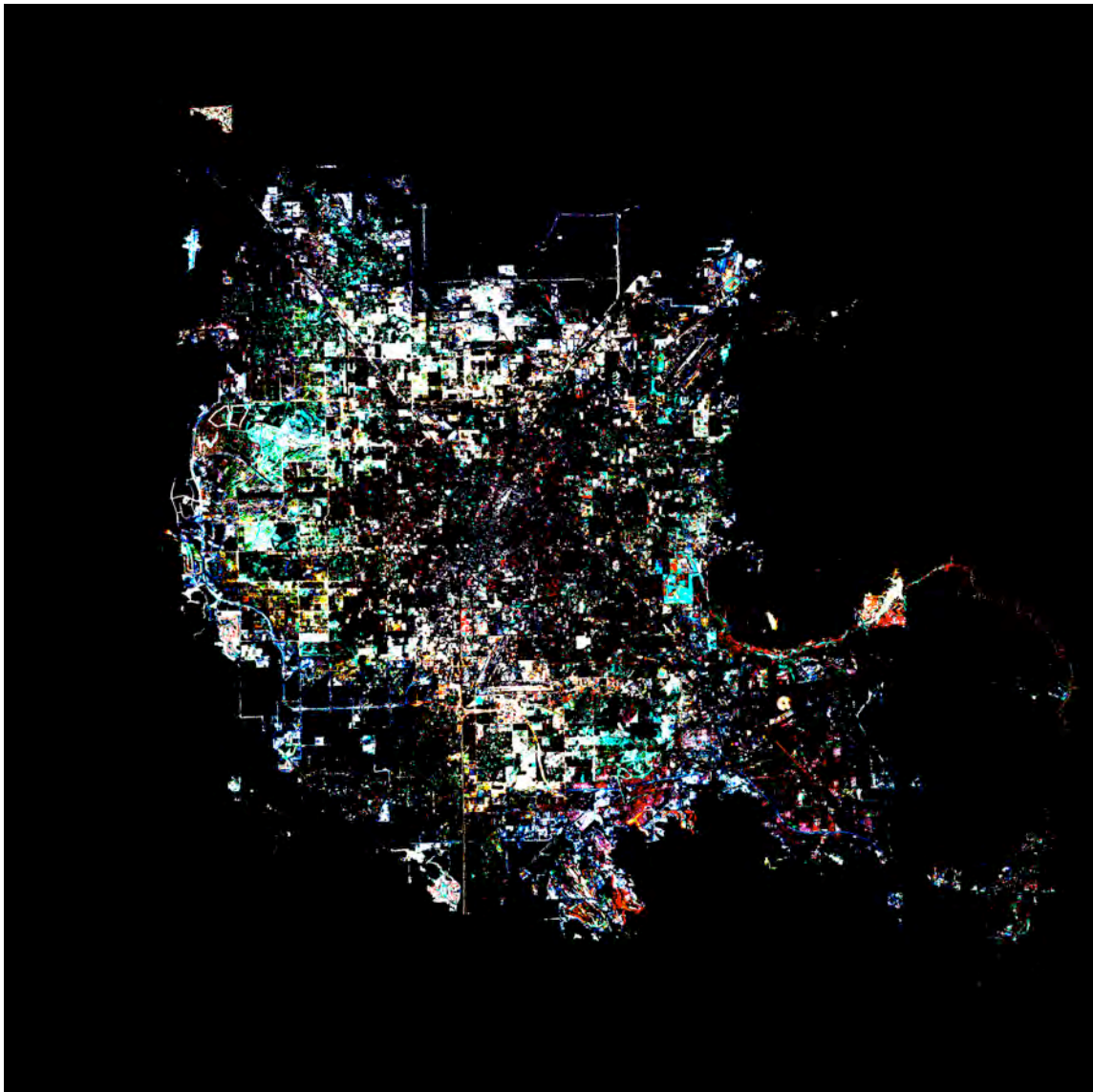


Figure 3.10 Image Differencing: False Color Composite

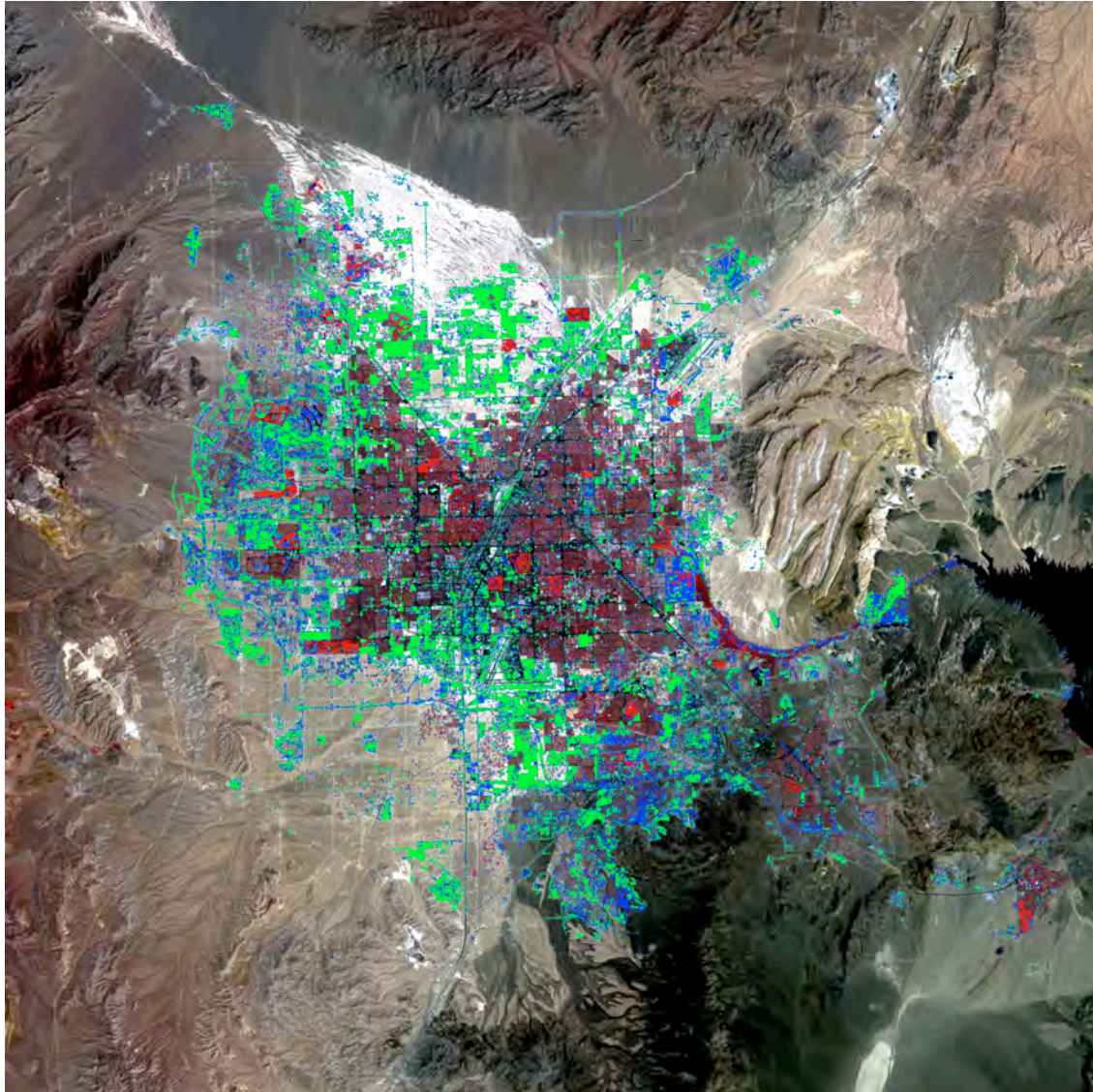


Figure 3.11 Image Differencing: Three Band Composite Image: Agree/Disagree Map

### (3.5.2) Image Ratioing

Image ratioing involves the division of the newer image by the older image, for  $n$  number of bands. Because you cannot divide the numerator  $(\text{Band } n)_{2000}$  by a denominator  $(\text{Band } n)_{1990}$  of zero, 0.01 was substituted for zero denominators. This value is sufficiently small that it did not significantly influence any results and it permitted the research to continue without throwing out pixels divided by zero. Values greater than 1.0

indicated that the 2000 image had higher reflectance while values less than 1 indicated that the 1990 image had higher reflectance. Values equal to 1.0 reflected equal reflectance between both years. Per the original distribution of each band (see Figure 3.12), it's clear that the ratio produced a non-normal distribution as expected from the literature review. To transform it to a more manageable distribution, the following transformation equation was applied:

$$\text{Transformed Value} = \text{atan}(\text{Band } i_{2000} / \text{Band } i_{1990}) + \Pi/4$$

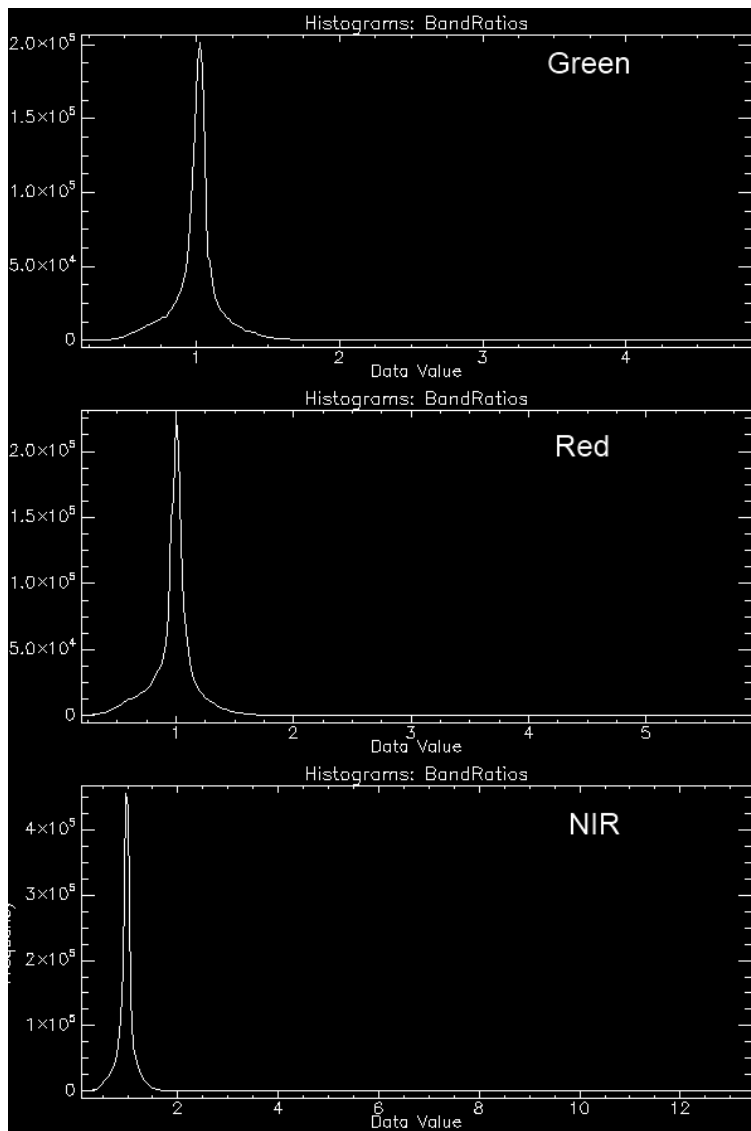


Figure 3.12 Image Ratioing: Original, Non-normal Distribution by Band

The theoretical purpose for this transformation is that arc tan returns a roughly linear distribution of values taken from  $1/x$  for all  $x$ 's within the bounds of 0 to 1. Values less than zero indicated that the 1990 image had higher reflectance while values greater than zero indicated that the 2000 image had higher reflectance. Values equal to 1 indicated equal reflectance for the two years. In Figure 3.13 we now see the distribution of each transformed band. Note that each distribution is now relatively normal, albeit peaked.

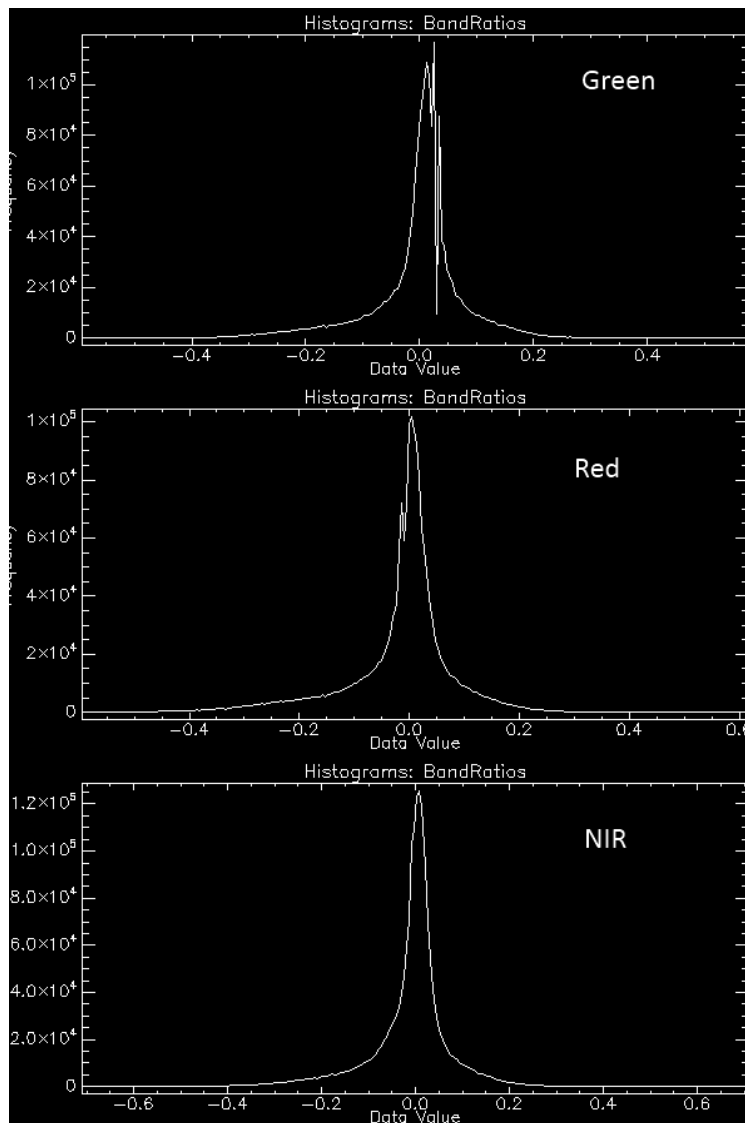


Figure 3.12 Image Ratioing: Arc tan Transformation Histograms by Band

One final transformation is applied by taking the absolute value of the previous arc tan transformation. An interesting note is the level of correlation between the three band ratios following the implementation of this transformation. In Figure 3.14 we see the correlation matrix reveals that each band has moderate to high correlation with the others.

Correlation	Green	Red	NIR
Green	1.0	0.96	0.8
Red	0.96	1.0	0.83
NIR	0.8	0.83	1.0

Figure 3.14 Image Ratio Correlation Matrix Using the Absolute Value of the Arctangent Transformation by Band

After these transformations, the three band ratios (green, red, NIR) had a range of possible values. Thresholds had to be set, unique to each band ratio, to determine areas of change/no change. The process used in threshold specification in image differencing is *identical* to the process applied for image ratioing. Following this process, two graphs were created to identify patterns. The first graph (see Figure 3.15) plotted the percent of accurately identified validation samples against the tested thresholds. Please note how regardless of which band, the percent of accurately identified validation samples follows the same pattern as the threshold increases. The second graph (see Figure 3.16) plotted the chi-square statistic against the tested thresholds and follows the same trend where, regardless of band, the chi-square statistic follows the same pattern as the threshold increases. The minimum chi-square statistic for each band and its associated threshold and % accuracy are shown in the table below (see Figure 3.17).

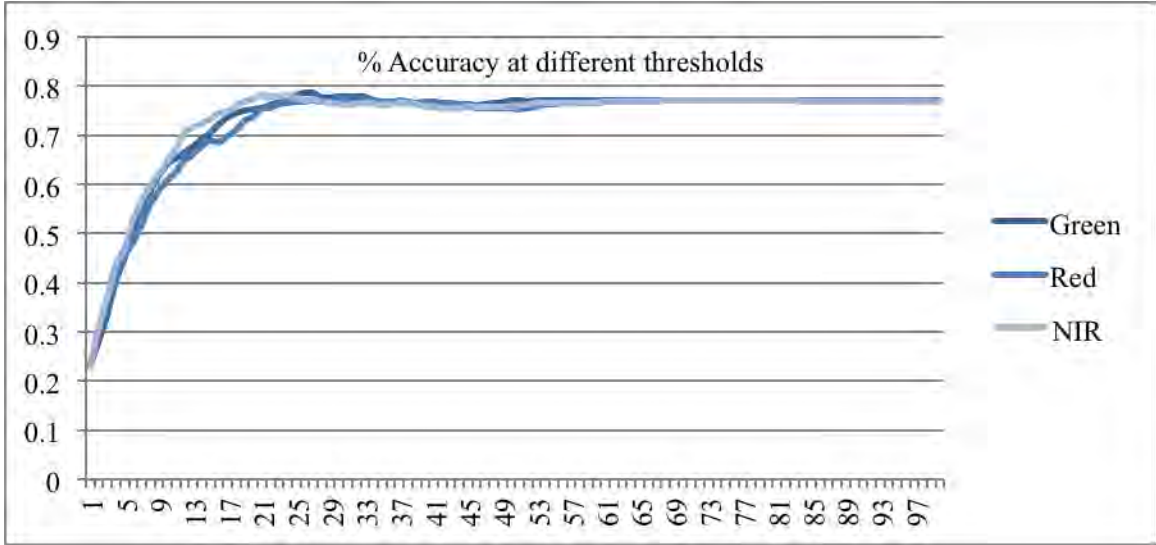


Figure 3.15 Image Ratioing: % Accuracy and Threshold

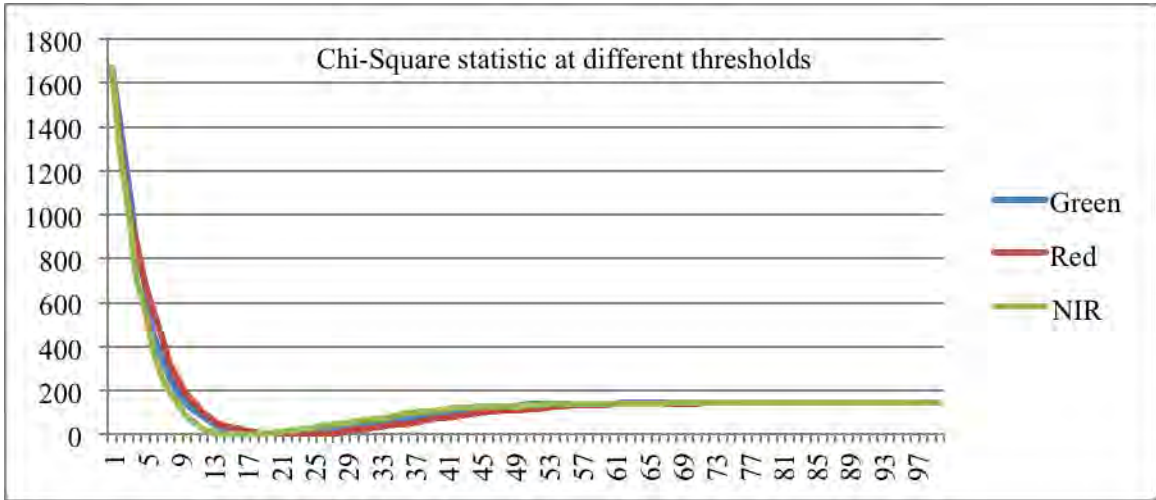


Figure 3.16 Chi-square Statistic and Threshold

	Threshold	Accuracy	Min (Chi-Squared)
Green	0.102	75%	0.102
Red	0.130	75.6%	0.045
NIR	0.114	74.8%	0.045

Figure 3.17 Image Ratioing Results

All three change maps were loaded to create a traditional false color composite image (see Figure 3.18). Intersecting the areas of change between the three maps produces areas of agreement (white) and areas of disagreement (colored). Additionally, a map composite image of all three change maps reflecting areas of agreement and disagreement only was also created (see Figure 3.19). Green indicates areas of agreement between the three change maps while blue indicates areas of disagreement. Using the principle of agree and disagree: this false color composite image of all three change maps reveals that all three change maps agree that 10.2% of the study area changed and disagree whether an additional 9.29% of the study area changed.

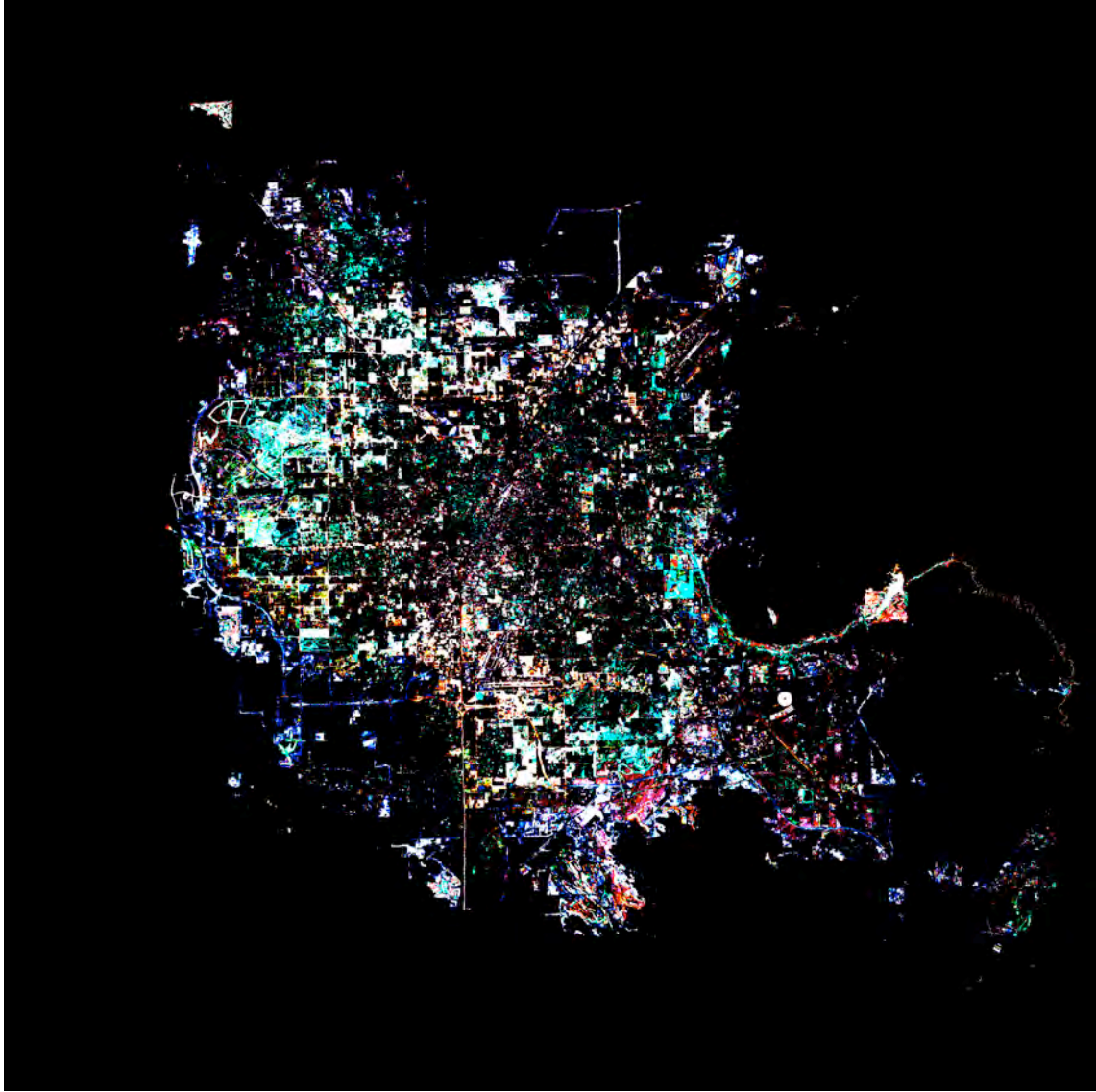


Figure 3.18 Image Ratioing: False Color Composite

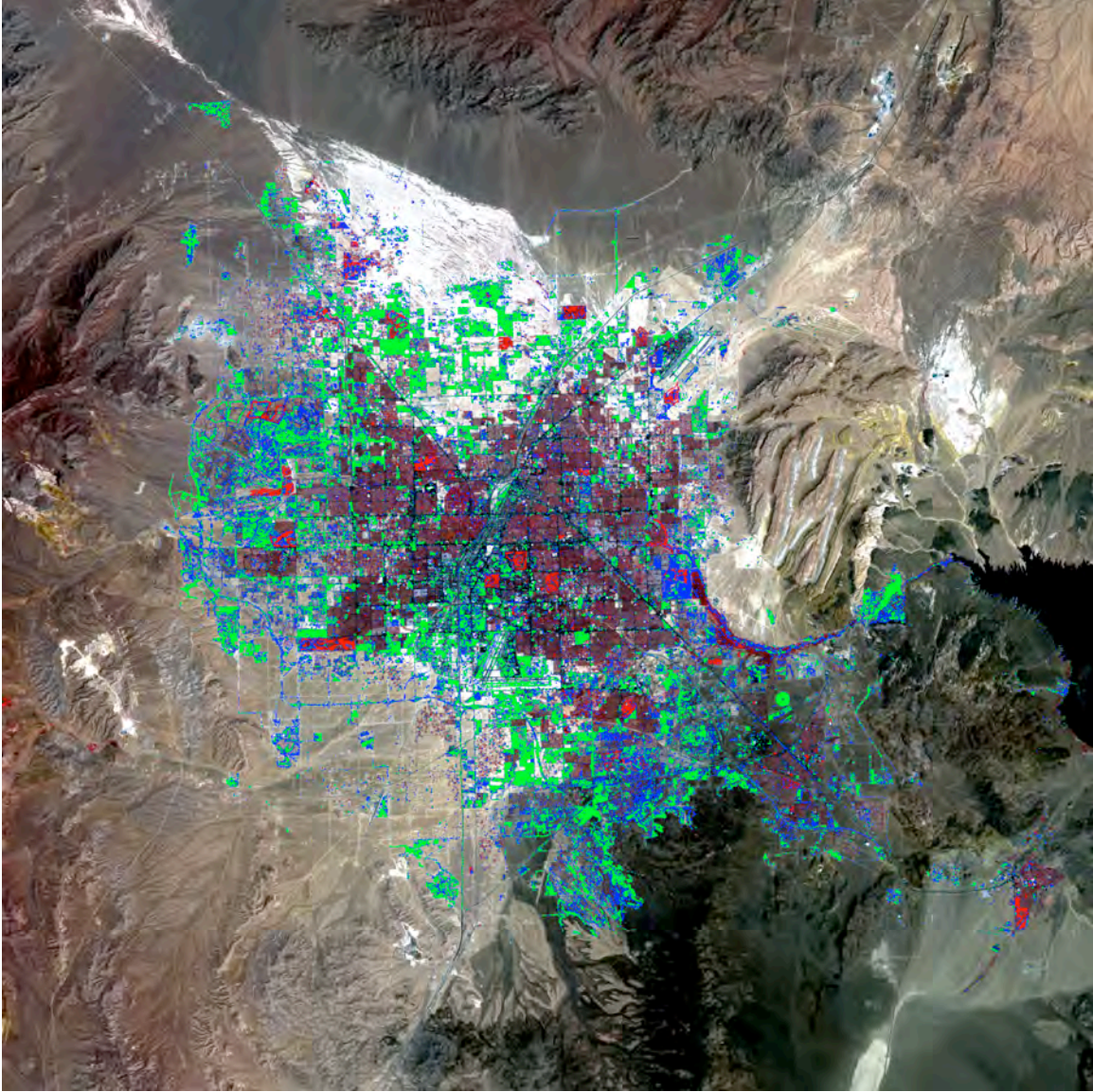


Figure 3.19 Image Ratioing: Three Band Composite Image: Agree/Disagree Map

### (3.5.3) Image Regression

As mentioned in the literature review, Image regression involves applying a linear regression model for each pair of bands between the two images using the pixels of Band<sub>1990</sub> as the independent (X) and the pixels of Band<sub>2000</sub> as the dependent (Y). The resulting regression equation is of the form:

$$\text{Predicted}_{2000} = \text{Band}_{1990} * m + b$$

where  $m$  is the slope and  $b$  is the intercept. Figure 3.20 details the equations for each band. The regression line was plotted on three scatter plots where the color scheme indicates density of points (see Figure 3.21, 3.22, 3.23).

Band	Slope ( $m$ )	Intercept ( $b$ )	R	$R^2$
Green	0.7958	0.0419	0.8154	0.6650
Red	0.7895	0.0460	0.8117	0.6589
NIR	0.8038	0.0569	0.8352	0.6975

Figure 3.20 Regression Equations by Band

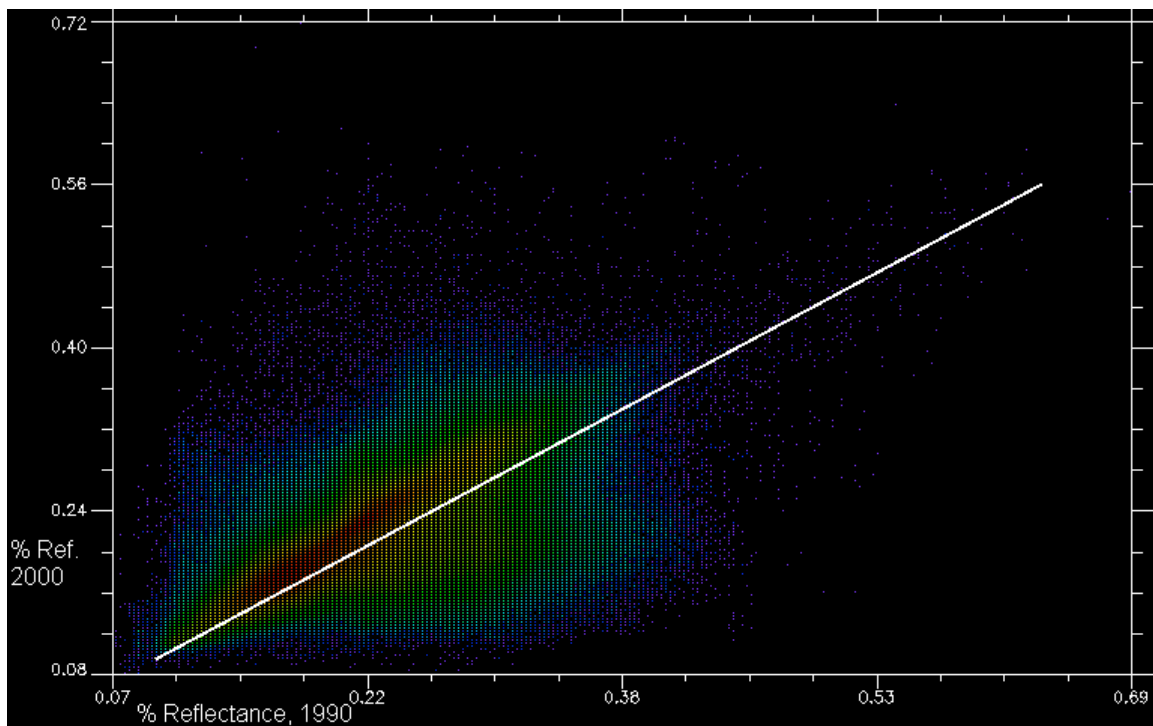


Figure 3.21 Regression Line for the Green Band

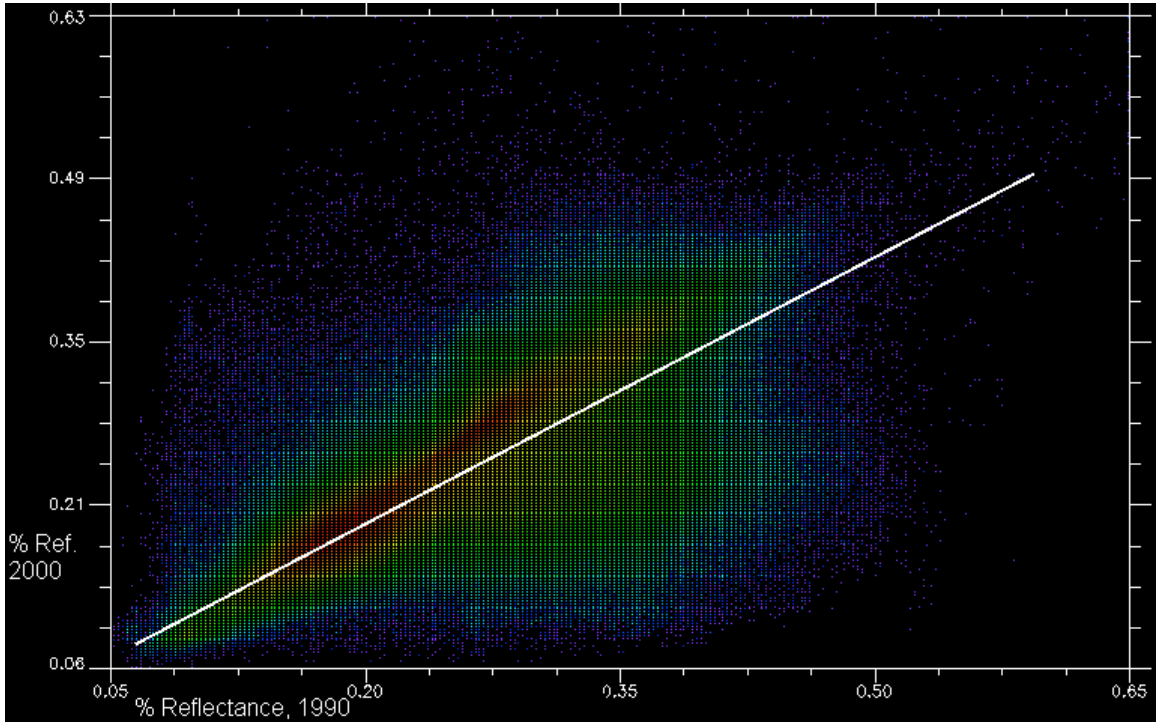


Figure 3.22 Regression Line for the Red Band

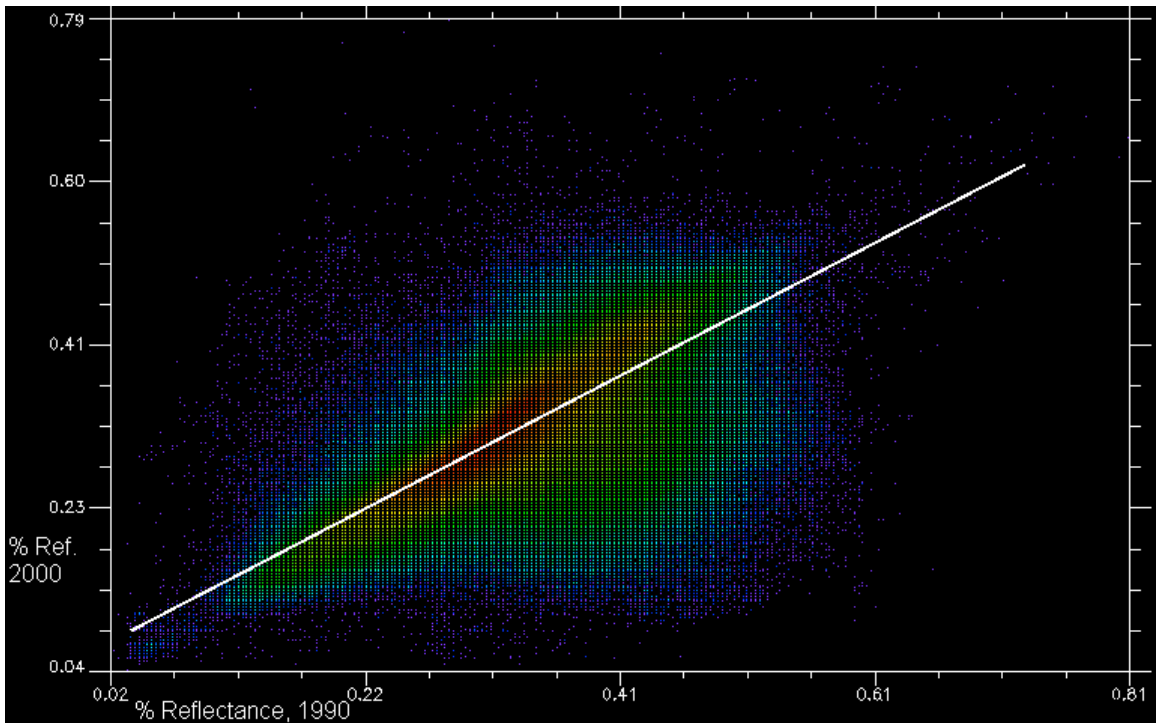
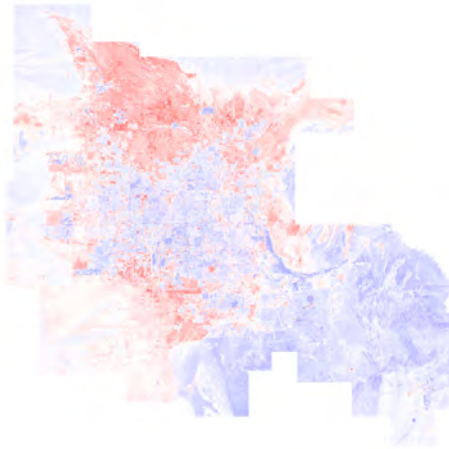


Figure 3.23 Regression Line for the NIR Band

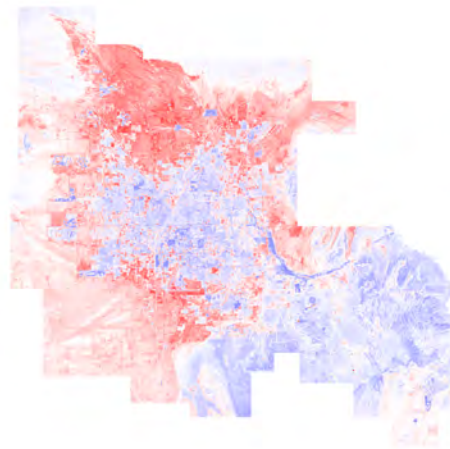
For each regression between band pairs, the residual (Re) was computed using:

$$Re = \text{Band}_{2000} - \text{Predicted}_{2000}$$

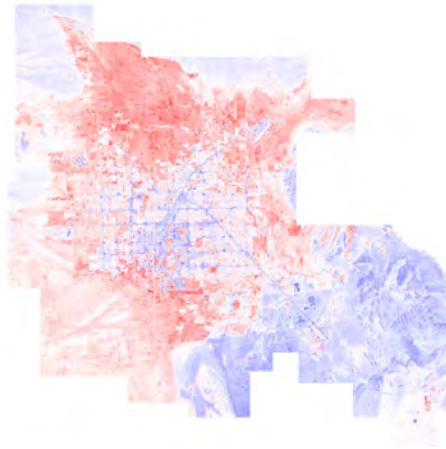
Values greater than zero signified that the regression under-predicted reflectance for the 2000 image while values less than zero signified that the regression over-predicted reflectance for the 2000 image. Values equaling zero indicated that the regression predicted reflectance for the 2000 image exactly (see Figure 3.24).



Green Residual Image



Red Residual Image



NIR Residual Image

Figure 3.24 Image Regression: Residual Images by Band  
Blue = residual < 0, White = residual = 0, Red = residual > 0

The residual images show that the regression over-predicted reflectance in the year 2000 in the southeast region of the study area where the terrain was more mountainous, providing a different spectral signature than the desert region in the northwest portion of the study area which indicated an under-prediction of reflectance for the year 2000. The desert in the northwest region contained drier soil composition than that of the southeast corner, and thus unique reflectance values for each region yielded different results from the regression equation. Additionally, weather reporting for this area for both years indicated no prior precipitation or change in pressure systems, indicative of weather patterns.

The histograms for these residuals were also plotted (see Figure 3.25).

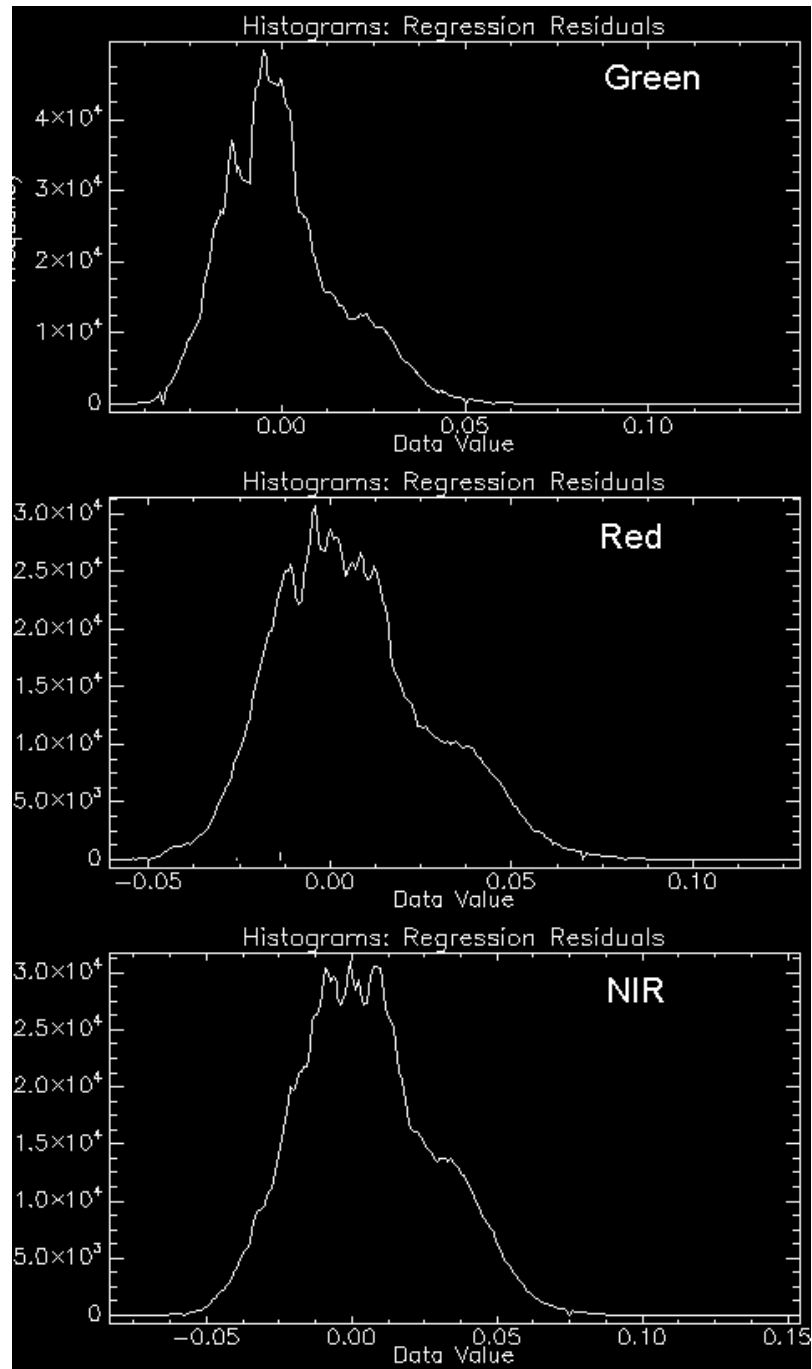


Figure 3.25 Image Regression: Histograms of the Residuals by Band

The absolute value of the residuals was then calculated. With the absolute value applied to the residuals, the values no longer reflect under or over-prediction of

reflectance, but the magnitude of the residual. Figure 3.26 gives an example of what a transformed histogram looks like using the Red band. Figures 3.27, 3.28, and 3.29 show the maps created from taking the absolute value of the residuals for the green, red, and NIR bands respectively. Figure 3.30 provides descriptive statistics for each band.

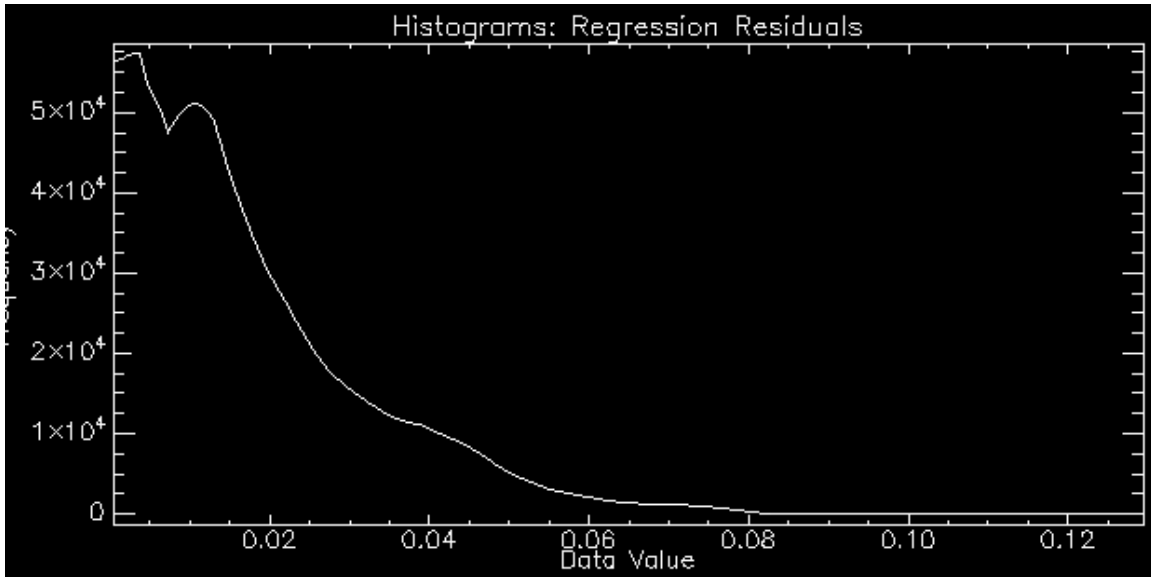


Figure 3.26 Image Regression: Histogram of the Absolute Value of the Residuals for the Red Band



Figure 3.27 Image Regression: The Absolute Value of the Residuals for the Green Band



Figure 3.28 Image Regression: The Absolute Value of the Residuals for the Red Band



Figure 3.29 Image Regression: The Absolute Value of the Residuals for the NIR Band

Band	Slope (m)	Intercept (b)	R	R <sup>2</sup>
Green	0.7958	0.0419	0.8154	0.6650
Red	0.7895	0.0460	0.8117	0.6589
NIR	0.8038	0.0569	0.8352	0.6975

Figure 3.30 Image Regression: Descriptive Statistics by Band

At this point, the three band residual images had a range of possible values. A threshold was selected, unique to each band ratio, to determine areas of change/no change. The method for selecting these thresholds is *identical* to the one applied to the previous change detection techniques. Figure 3.31 plotted the percent of accurately identified validation samples against the tested thresholds and Figure 3.32 plotted the chi-square statistic against the tested thresholds. Please note how regardless of which band, the percent of accurately identified validation samples in the first graph follows the same pattern as the threshold increases while the second graph also follows the same trend where, regardless of band, the chi-square statistic follows the same pattern as the threshold increases. The minimum chi-square statistic for each band and its associated threshold and % accuracy are shown in the table below (see Figure 3.33).

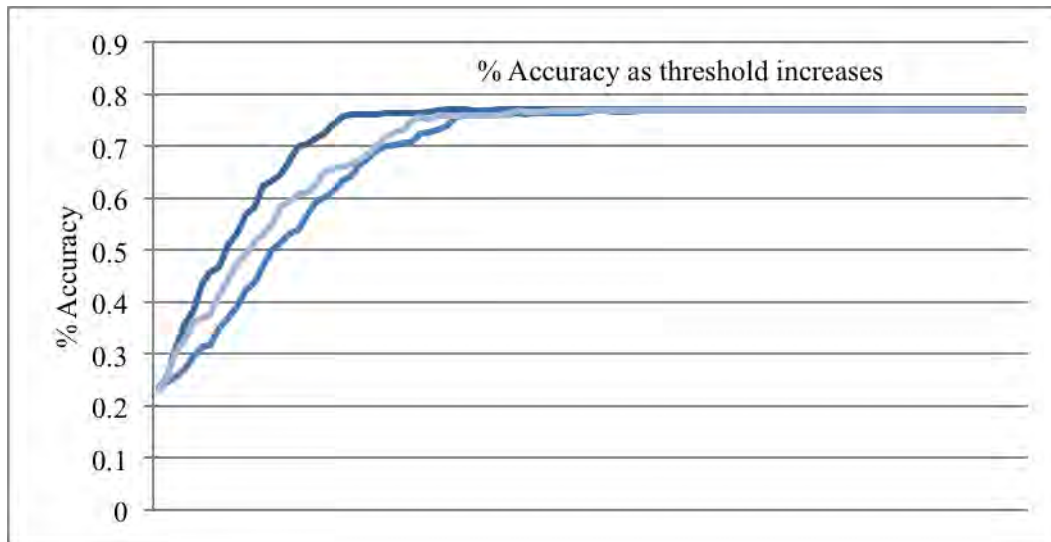


Figure 3.31 Image Regression: % Accuracy and Threshold

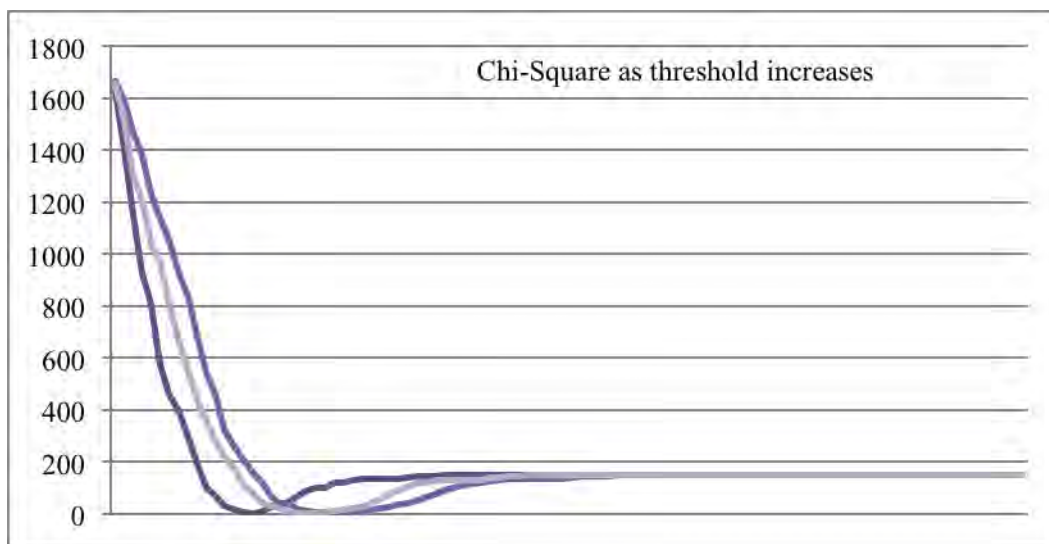


Figure 3.32 Image Regression: Chi-square Statistic and Threshold

Band	Threshold	Accuracy	Min (Chi-Squared)
Green	0.0215	67.2%	0.045
Red	0.0301	66.4%	0.045
NIR	0.0327	66%	0.181

Figure 3.33 Image Regression Results

All three change maps were loaded to create a traditional false color composite image (see Figure 3.34). Intersecting the areas of change between the three maps produces areas of agreement (white) and areas of disagreement (colored). Additionally, a map composite image of all three change maps reflecting areas of agreement and disagreement only was also created (see Figure 3.35). Green indicates areas of agreement between the three change maps while blue indicates areas of disagreement. Using the principle of agree and disagree: this false color composite image of all three change maps reveals that all three change maps agree that 12.5% of the study area changed and

disagree whether an additional 10.1% of the study area changed.



Figure 3.34 Image Regression: False Color Composite

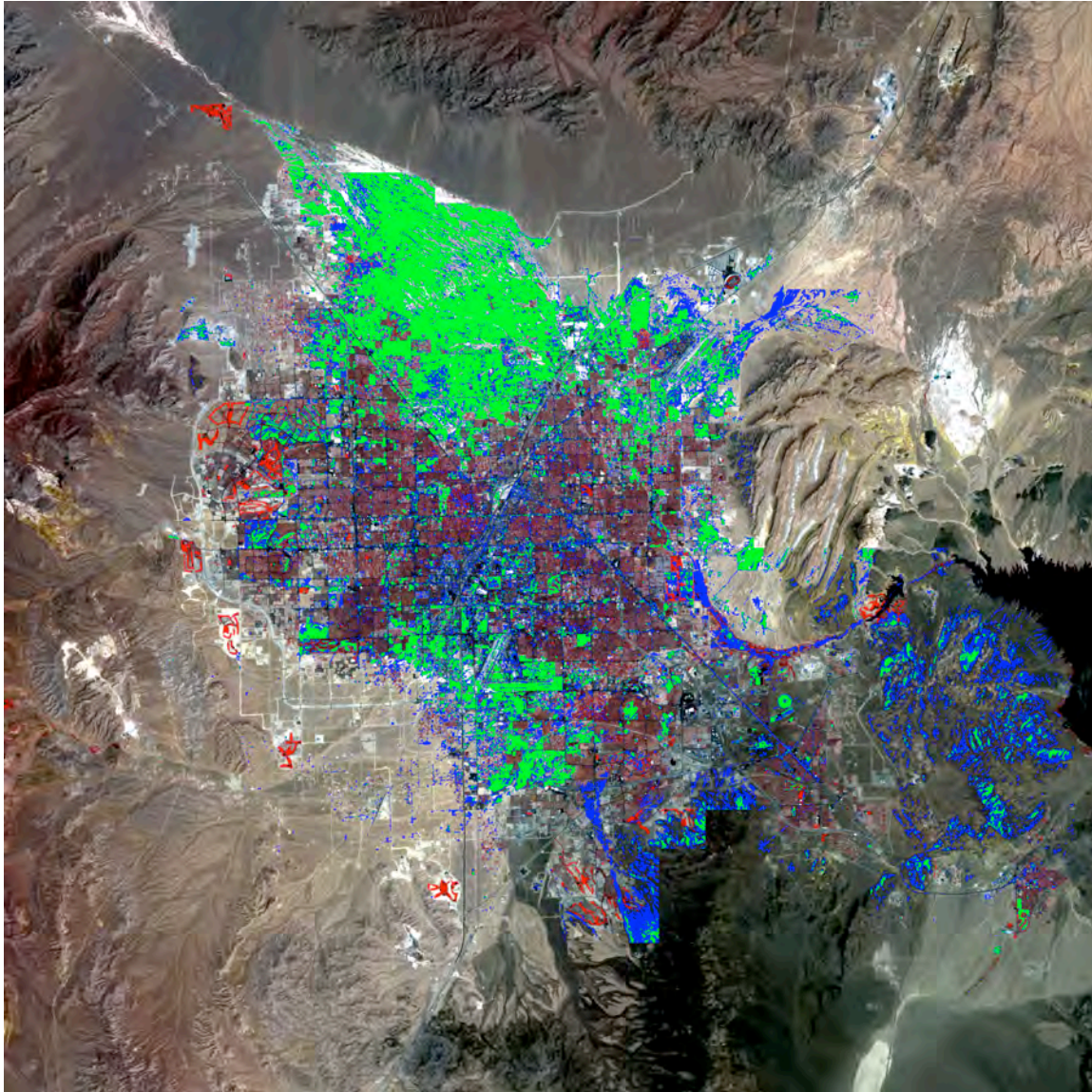


Figure 3.35 Image Regression: Three Band Composite Image: Agree/Disagree Map

#### (3.5.4) *Vegetation Index Differencing*

Vegetation index differencing involves a form of band ratioing. The first step of this technique yields the Normalized Difference Vegetation Index (NDVI) as calculated on each image using the following formula:

$$\text{NDVI} = (\text{NIR} - \text{Red}) / (\text{NIR} + \text{Red})$$

NDVI output values range between -1 and 1 and can be seen in Figure 3.36 and

3.37 where red indicated an NDVI below zero, green indicated an NDVI above zero, and black indicated an NDVI equal to 1.

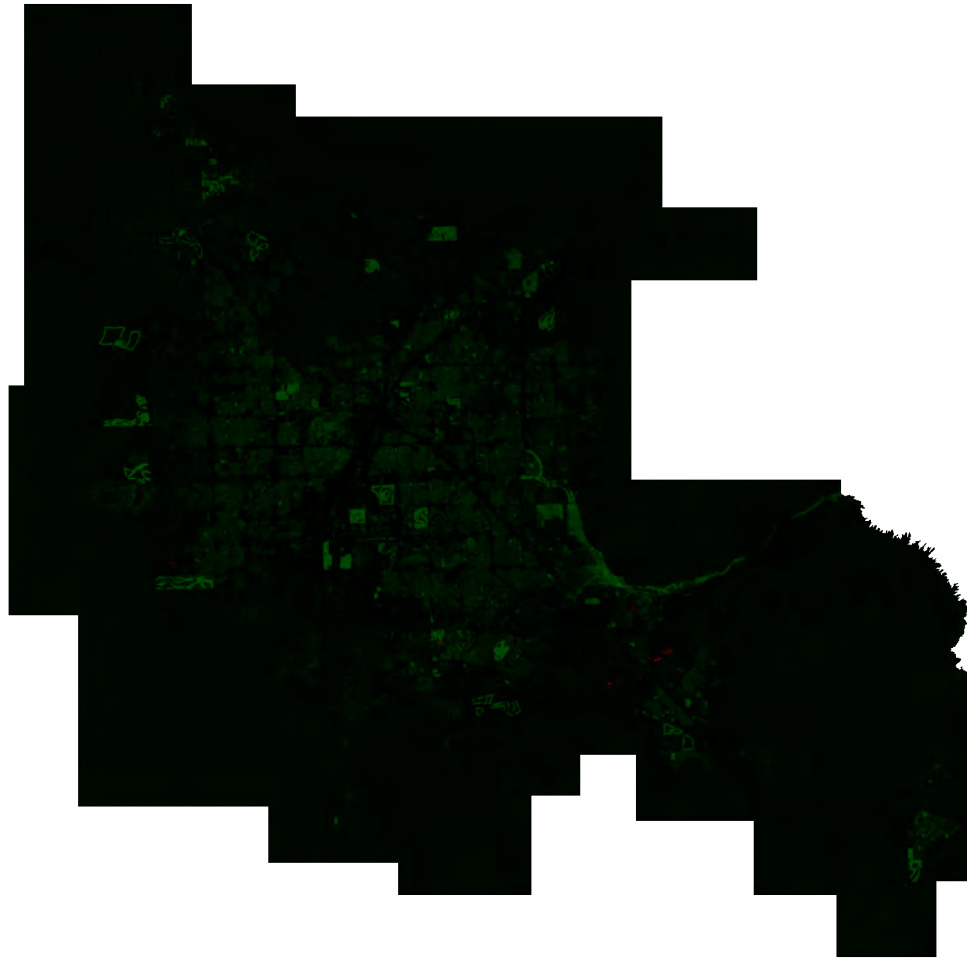


Figure 3.36 NDVI Values for 1990

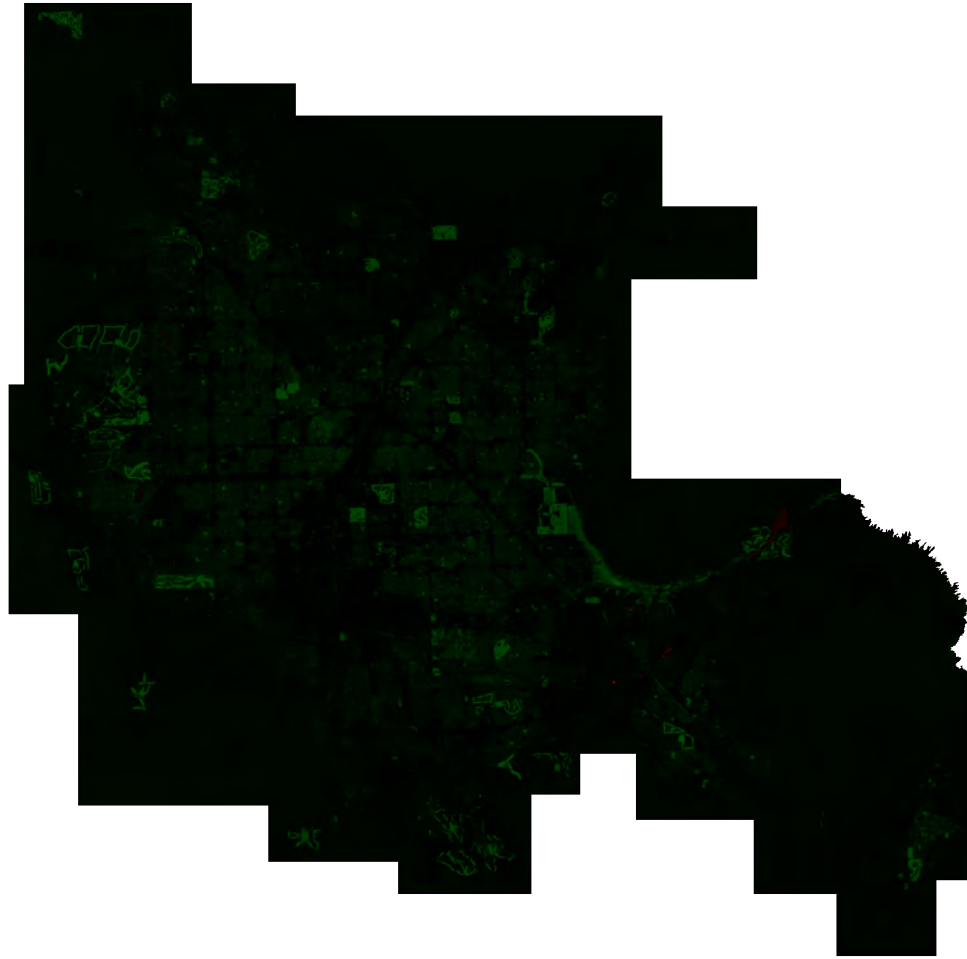


Figure 3.37 NDVI Values for 2000

The second step in this method requires the calculation of the NDVI difference (D) between the two dates:

$$D = NDVI_{2000} - NDVI_{1999}$$

The difference output ranges between -2 and 2 where positive values indicated an

increase in NDVI since 1990 and negative values indicated a decrease in NDVI since 1990. Figure 3.38 is the NDVI difference map where red indicates a decrease in NDVI, green indicates an increase in NDVI, and black indicates no change in NDVI.



Figure 3.38 NDVI Difference

Finally, the absolute value of the difference image between the two dates was calculated. The maximum and minimum value of this layer is 0 and 2. Positive values

indicated a magnitude of change in NDVI. Figure 3.39 shows the absolute value of the NDVI difference values where black indicates no change in NDVI and higher levels of gray indicate higher absolute difference in NDVI.



Figure 3.39 NDVI Absolute Difference

In Figure 3.40, the NDVI absolute difference histogram was plotted with Frequency along the Y-axis and absolute difference of NDVI along the X-axis. Figure 3.41 provides descriptive statistics to detail the absolute change in NDVI since 1990.

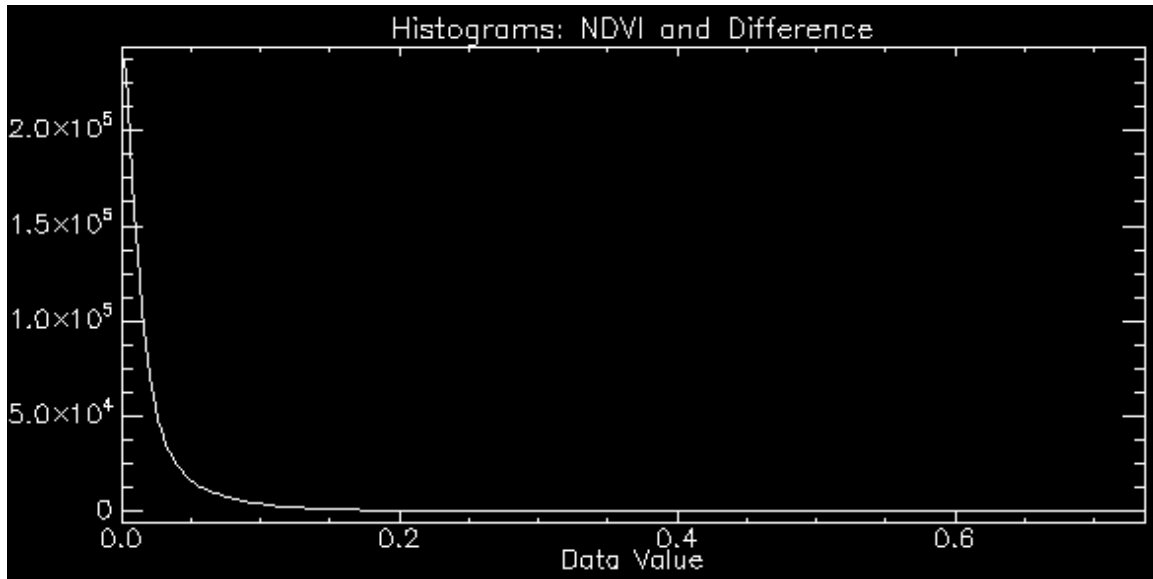


Figure 3.40 NDVI Absolute Difference Histogram

Minimum	Maximum	Average	Standard Deviation
0.0	0.7395	0.0293	0.0556

Figure 3.41 Descriptive Statistics of Absolute Difference in NDVI since 1990

At this point the selection of a threshold is necessary to determine areas of change/no change in the absolute difference in NDVI data. To determine which threshold was best, one hundred different thresholds between the minimum and the maximum value of the layer were examined and the accuracy of each threshold at identifying change (among the calibration points) was recorded. To determine the final accuracy for reporting, we looked at how well our change map identified our validation samples. The threshold that best classified our validation samples was 0.495 with an accuracy of 77%

(see Figure 3.42) where green indicated a changed area.

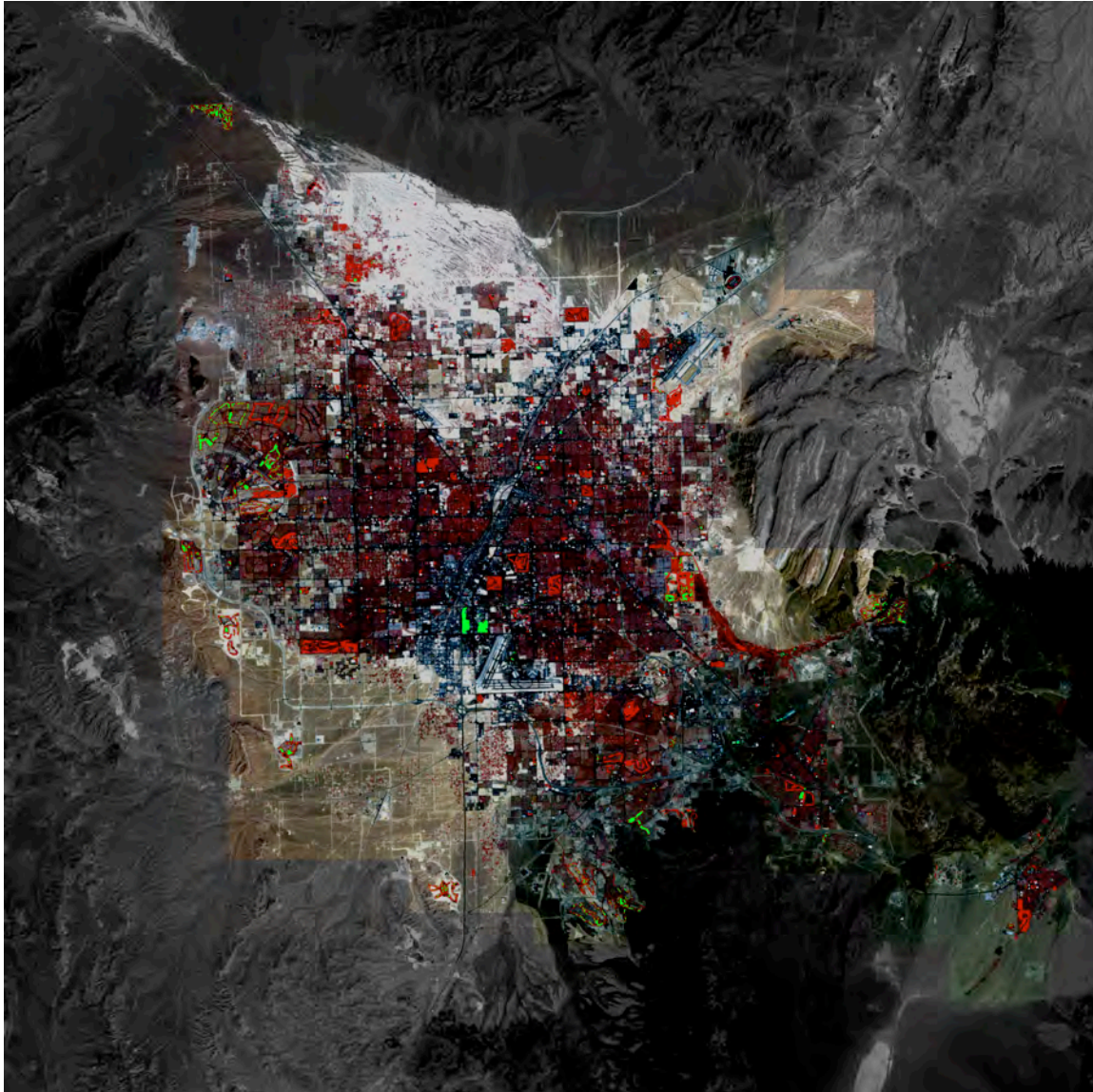


Figure 3.42 Vegetation Index Differencing: “Best Change” Map  
This “best change” map reflects the highest amount of accuracy at 77% with a threshold of 0.495.

However, it is of note that moving the threshold higher than 0.495 did not influence the accuracy much (see Figure 3.43). Within our validation dataset, 23% of the points were marked as changed pixels. Because our measure of accuracy for change maps

is percent of accurately identified validation samples, it is possible to classify *all* pixels in our image as no change and *still* reach a relatively high accuracy of 77% using the validation set. While this method of reaching the best change/no change threshold is an honest statistic, it does not meet our standard. This is notable since it is the same phenomena that would occur with all the change detection methods in this study, i.e. 77% accuracy by classifying *all* pixels as no change. As a result, another approach to selecting a threshold has been applied to all change detection techniques in this study.

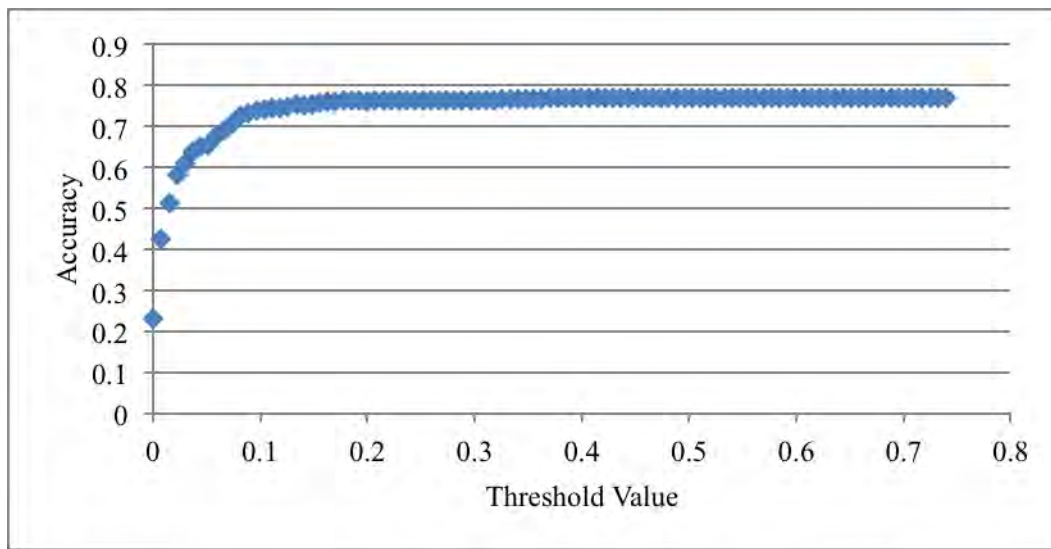


Figure 3.43 Vegetation Index Differencing: % Accuracy and Threshold

Like the other change detection methods, a threshold must be set to determine what is change and no change. For example, all values  $> 0.185$  were classified as change (see Figure 3.44). The method for selecting these thresholds was *identical* to the one applied to the previous change detection techniques. After examination of the chi-square statistic, a local minimum at the threshold of 0.052 was identified. This means that the distribution of observed and actual changes were approximately the same (see Figure 3.45).

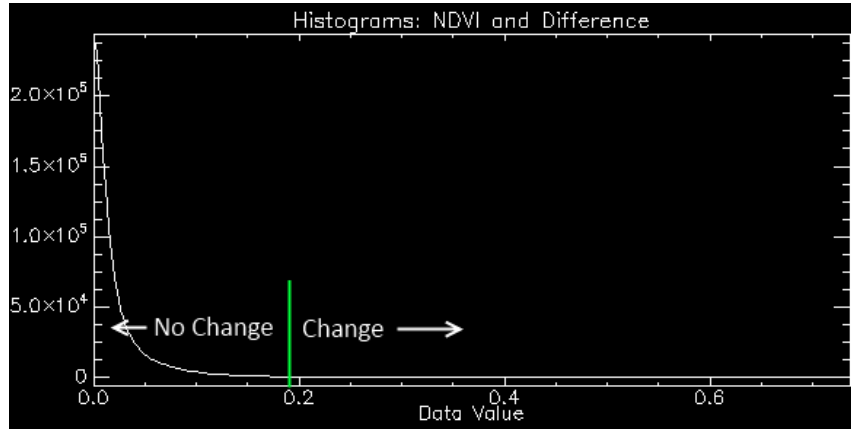


Figure 3.44 Vegetation Index Differencing: Setting a Threshold

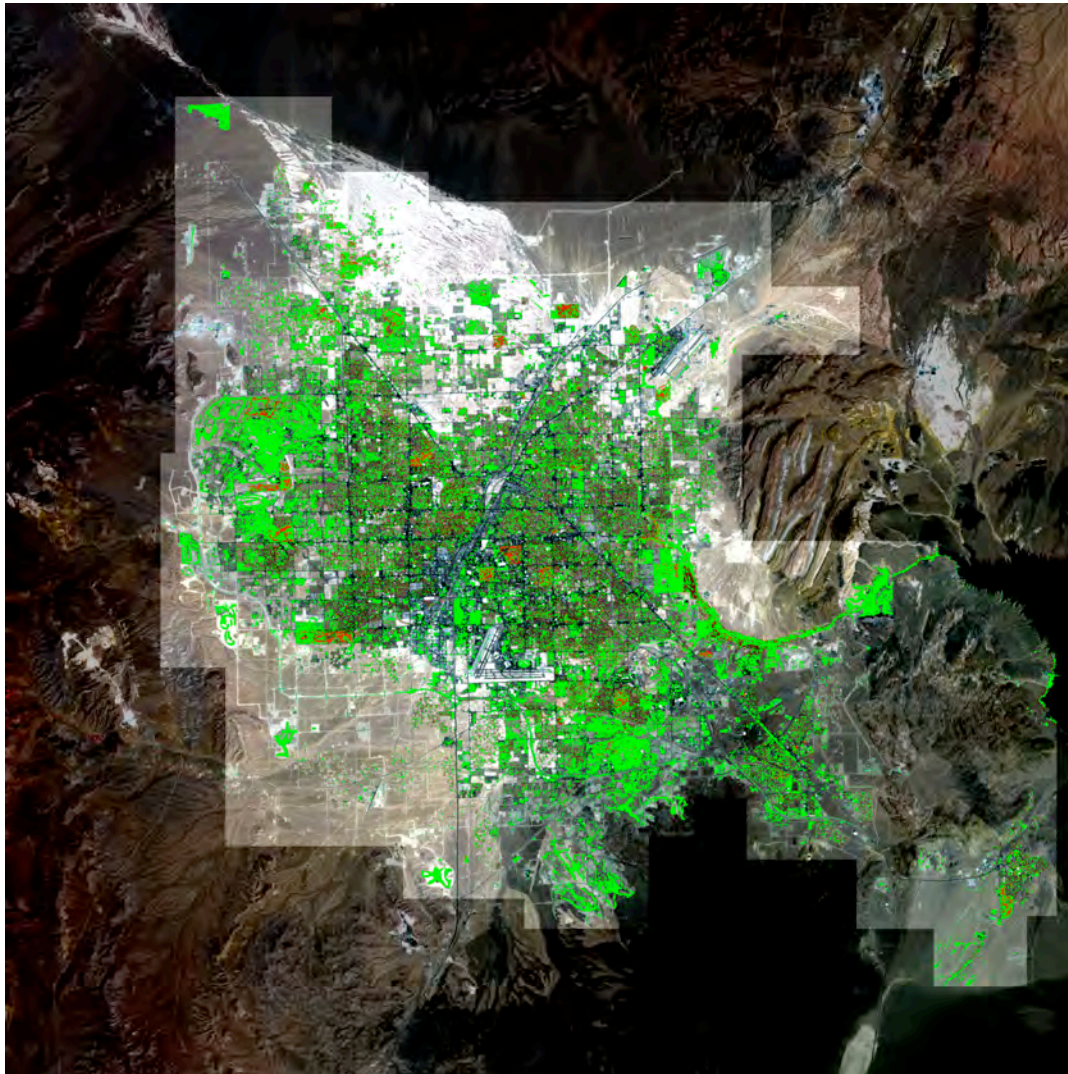


Figure 3.45 Vegetation Index Differencing:  
“Best Change” Map Using Chi-square Statistic

This “best change” map reflects the highest amount of accuracy at 65% with a threshold of 0.052. While the accuracy of the “best change” map using the chi-square statistic to select a threshold is lower than hoped for, the distribution of changed pixels in the map more closely followed that of the validation samples. This is preferable over the 77% “best change map” that assigns *all* pixels to no change. A visual comparison of Figure 3.42 and 3.45 clearly confirms the choice to use the chi-squared statistic in selecting a threshold for all change detection techniques in this study.

#### (3.5.5) *Principal Components Analysis*

Principal components analysis (PCA) involves combining the green, red, and NIR bands for each image into a single stacked dataset. Of the new dataset, bands 1-3 were from 1990 and bands 4-6 were from 2000. Using ENVI geospatial image processing software, PCA was run on the stacked image. In Figure 3.46 values less than zero indicated a negative loading on the component and values greater than zero indicated a positive loading on the component. Values equaling zero indicated no loading on the component. It is of note that each component’s distribution is centered on zero.

With PCA layers, the selection of two thresholds was required to identify change (see Figure 3.47). Each PCA layer was transformed by taking the absolute value of the component. This allows the setting of a single threshold on each band to determine change. Figure 3.48 shows the absolute value component histograms where values that equal zero indicated no loading on the component and values greater than zero indicated the magnitude of loading on the component.

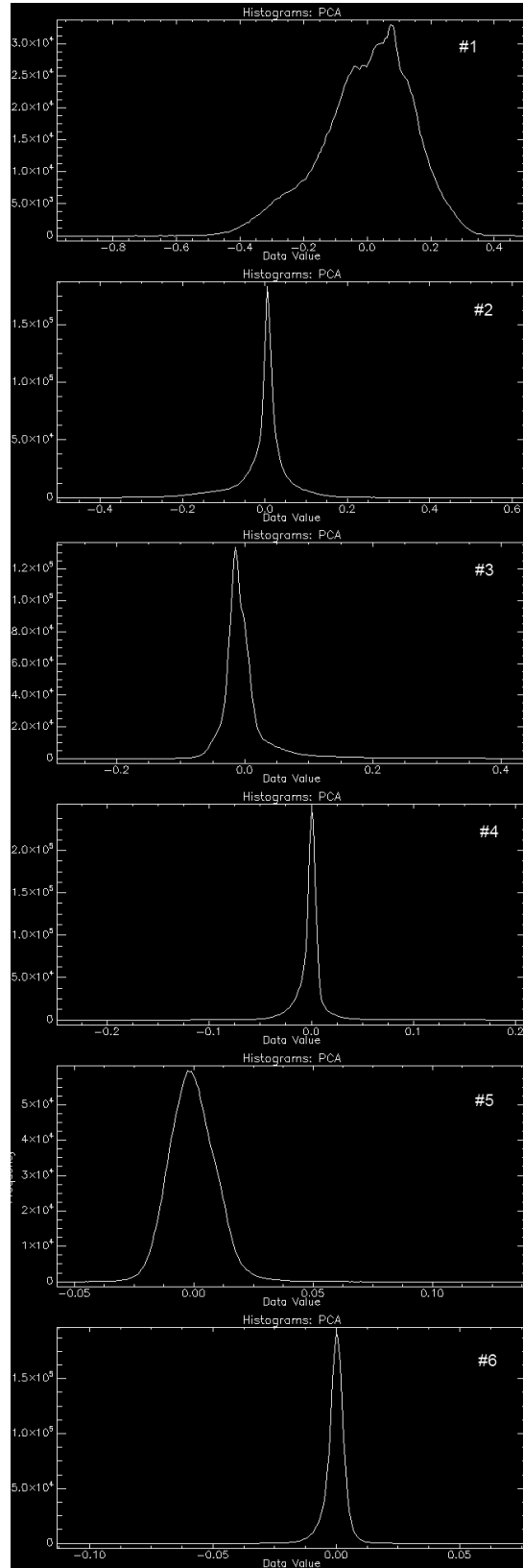


Figure 3.46 PCA: Component Histograms

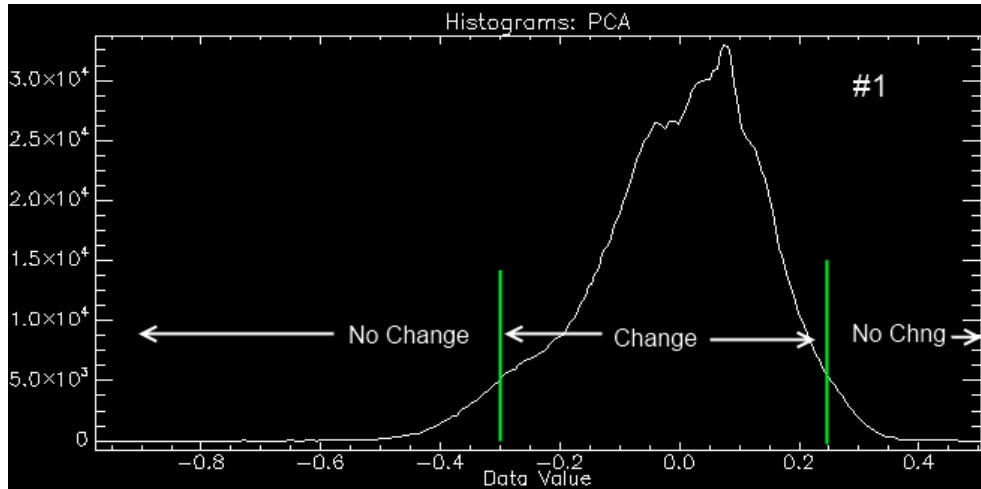


Figure 3.47 Setting Two Thresholds for PCA Layers

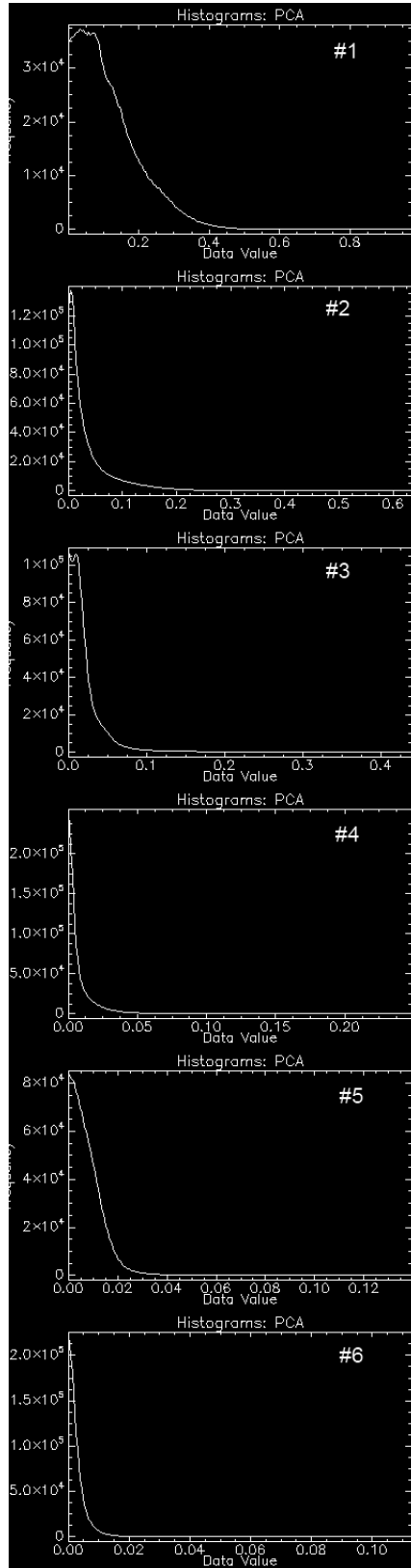


Figure 3.48 PCA: Absolute Value Histograms by Component

After these transformations, the three components have a range of possible values. A threshold had to be set, unique to each component, to determine areas of change/no change. The method for selecting these thresholds was identical to the one applied to the previous change detection techniques. Two graphs were created to identify patterns where Figure 3.49 plotted the percent of accurately identified validation samples against the tested thresholds and Figure 3.50 plotted the chi-square statistic against the tested thresholds. The minimum chi-squared statistic for each component and its associated threshold and % accuracy are shown in the table below (see Figure 3.51).

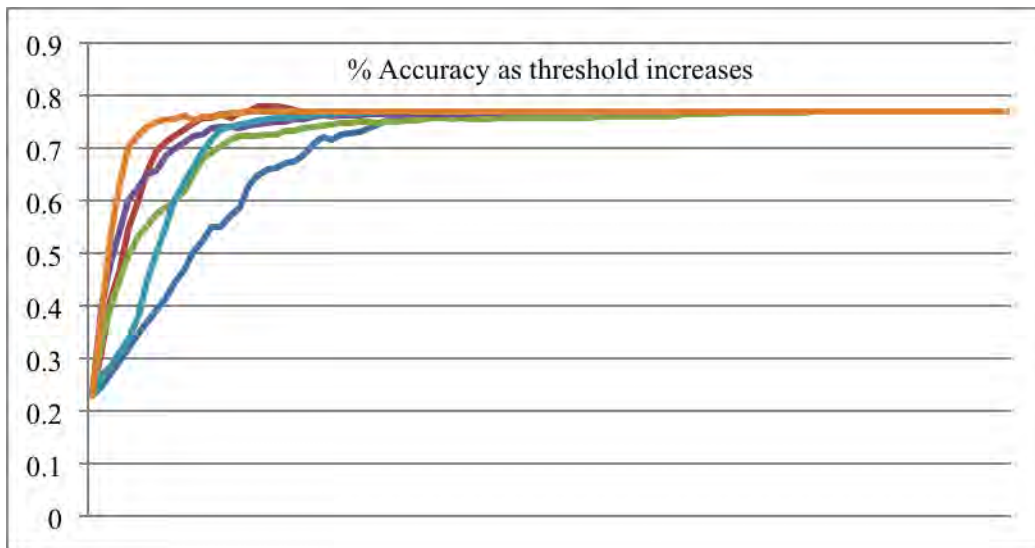


Figure 3.49 PCA: % Accuracy and Threshold

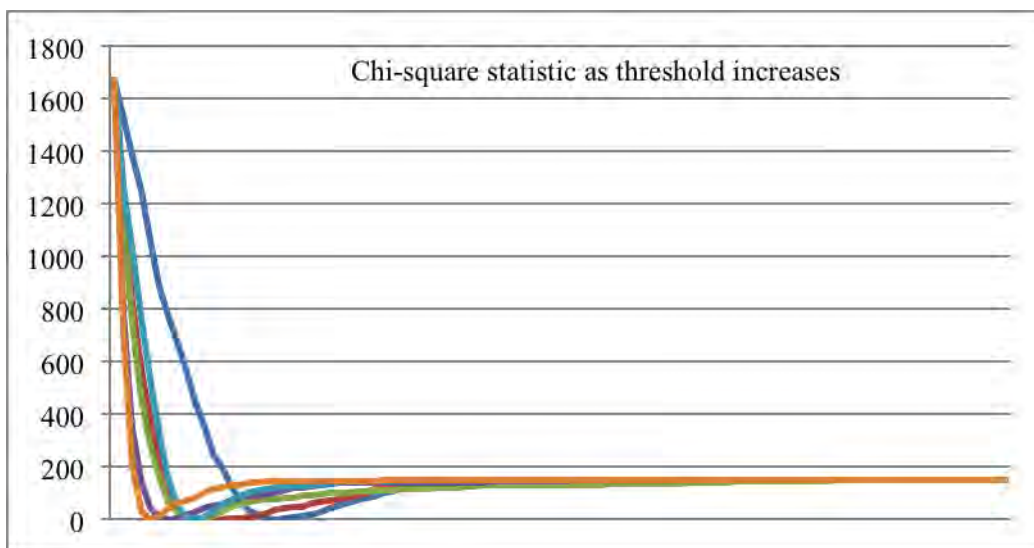


Figure 3.50 PCA: Chi-square Statistic and Threshold

Components	Threshold	Accuracy	Minimum Chi-Square
1	0.1760	64.8%	0.0452
2	0.0700	74.6%	0.1016
3	0.0441	61.8%	0.9147
4	0.0149	65%	1.3665
5	0.0126	60%	0.7228
6	0.0045	70.2%	0.0113

Figure 3.51 Principal Components Analysis Results

From the table above, clearly the second component and the sixth component are the best components at predicting change. Using the thresholds in the table above, two change maps were created for the second and sixth component (see Figure 3.52 and 3.53) where white reflects areas of change and black reflect areas of no change. A visual inspection of the two change maps concludes that the second component provides the

best map of change.

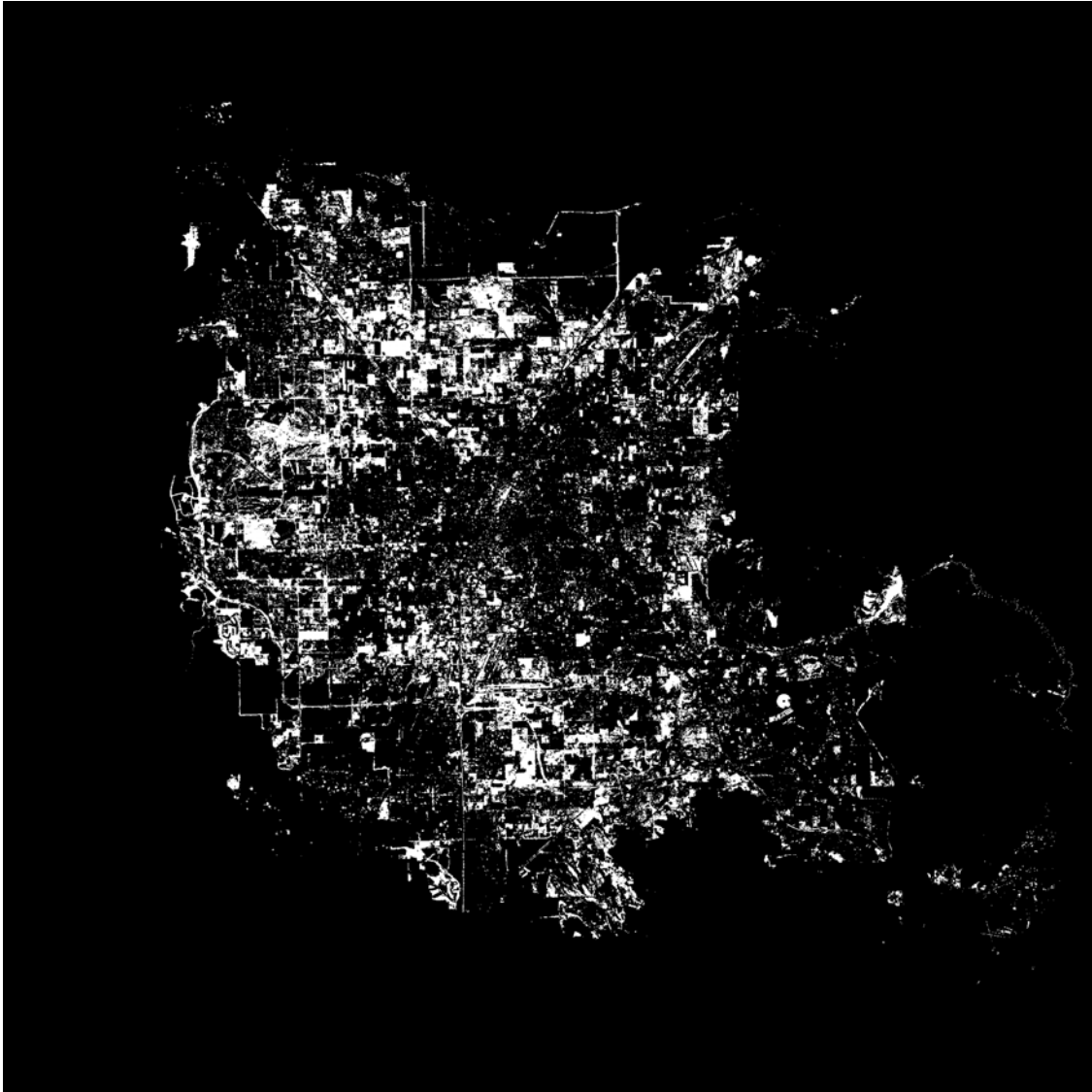


Figure 3.52 PCA Second Component Change Map  
This second component change map  
reflects the ability to predict change with 74.6% accuracy.

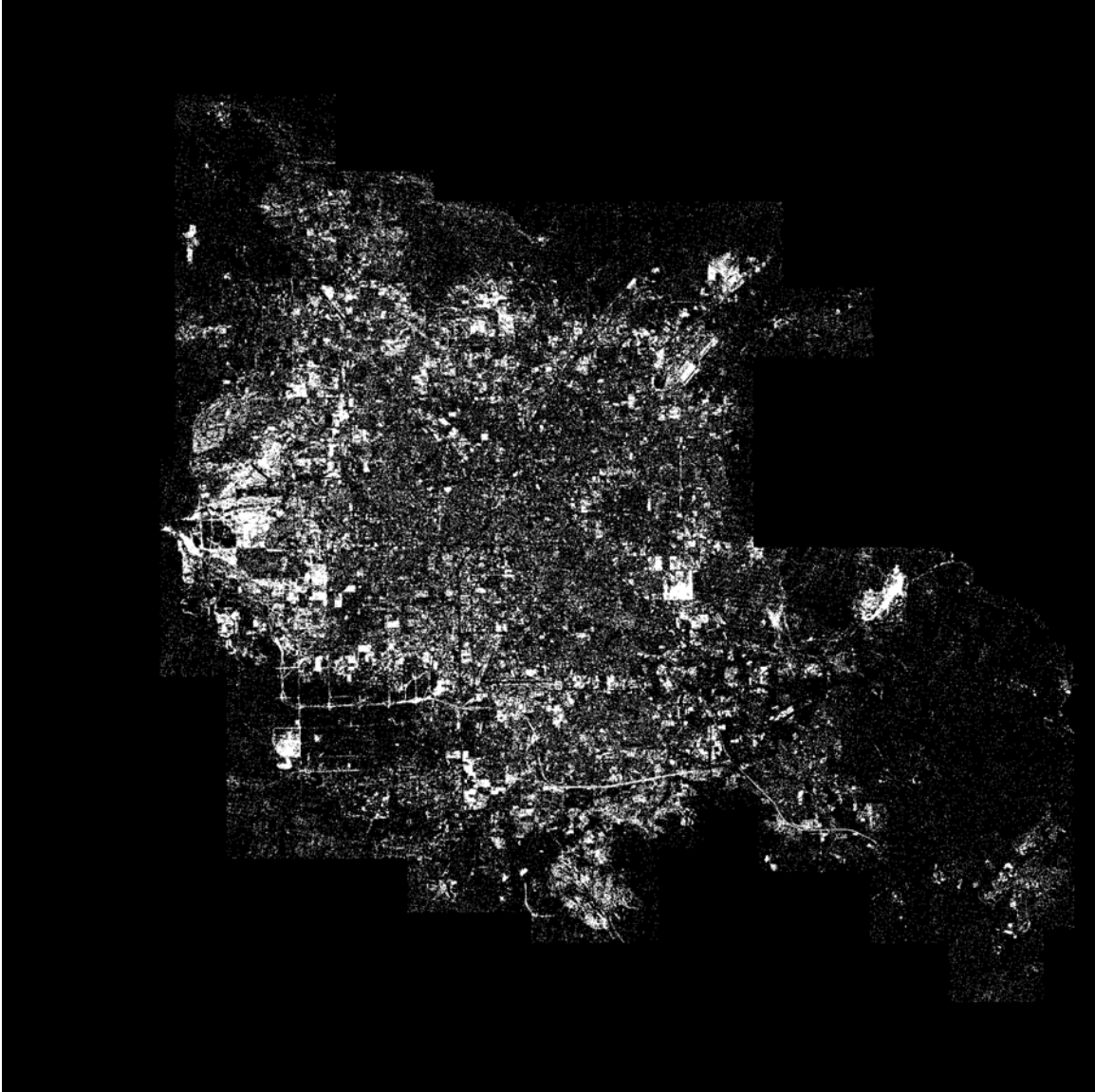


Figure 3.53 PCA Sixth Component Change Map  
This sixth component change map  
reflects the ability to predict change with 70.2% accuracy.

### (3.6) Discussion of Results

After a thorough execution of each change detection method, it was clear that the determination of thresholds for each technique was critical to method success. This will be discussed in the next chapter.

## Chapter 4: Discussion and Conclusion

This research was designed to use satellite remote sensing technology in combination with a variety of change detection methods to detect, measure, and map urban growth of the greater Las Vegas area between 1990 and 2000. The research began with the working hypothesis that while all of the methods tested would detect major change within the study area, the change threshold specification required by each method would be a significant subjective complication of the work. In other words, each method would require a subjective decision to be made of the practitioner as to what degree of change (as numerically measured by the method) constituted genuine change on the ground.

With the context of this working hypothesis and the change specification problem, this thesis addressed the following three objectives:

1. To assess urban change in Las Vegas between 1990 and 2000 using five change detection methods popular in satellite remote sensing.
2. To compare the results of the five change detection methods by first, determining the success of the method in capturing change between 1990 and 2000 and second, determining how well each method performed relative to each other.
3. To address the problem of change threshold specification by introducing a simple computer method whereby that specification could be done objectively.

While the first objective of this thesis has already been achieved as described in detail in the previous chapter, the other two objectives require more conclusive comment.

### (4.1) Objective 2: Comparing the Methods

- *Image differencing.* In terms of overall accuracy, this change detection method provided excellent performance. It is significant that the accuracy of the method was not impacted by the choice of bands. This fact is comforting since band selection has always been a source of some anxiety to the change detection researcher. As a visual comparison of the absolute value difference images demonstrates, the spatial distribution of the errors in the method is also consistent from band to band. Additionally, looking at the agree/disagree image, it follows the pattern of change expected in the study area. There were no large patches of false positives or missed change that came as a surprise.
- *Image ratioing.* Once the image ratio was transformed mathematically so that a single change threshold value could be used (rather than a pair), the remainder of the analytical process for detecting change was nearly identical to both image differencing and vegetation index differencing. This minor additional step, which was quite intuitive to us, has not been recorded in the change detection literature. Of all the change detection methods, image ratioing was superior when overall accuracy is the metric of goodness. However, unlike image differencing, the accuracy was impacted by the choice of band.
- *Image regression.* Compared to the other methods, the accuracy of the image regression approach was disappointingly low. The pattern of error was also a big problem since it was spatially dependent (large areas of error) rather than randomly distributed (small patches of error). In large measure, this spatial dependence of error was due to the distribution of vegetation in the study area. For example, the method shows that the White Rock Desert north of Las Vegas

was dramatically modified between 1990 and 2000. This faulty depiction was encountered regardless of the image bands used in the regression. This significant geographical error was due to the difference in vegetation greenness, and/or soil moisture differences in the two sample years. It was not the substantive effect of urbanization. We are at a loss to describe why the regression approach was so sensitive to this vegetation change when the ratio methods were not. More research into this problem is warranted.

- *Vegetation index differencing.* After review of the “best change” vegetation index differenced maps, it was clear the chi-square map was the best among them, especially for explaining the variability of change/no change in the study area. The alternative measure of agreement created a map that under-predicted change at a level too great to make it useful in a practical sense. The best threshold for this method was 0.052, which accurately placed 65% of the validation samples into the correct change/no change category. While even the accuracy of the best vegetation index differenced map was poor in comparison to the maps produced by ratioing and differencing, the spatial distribution of changed pixels in the map more closely followed that of the validation samples. From an accuracy assessment perspective, this would be preferable to a hypothetical map that might possess higher overall accuracy (e.g. 75%) but have poor power to detect change, i.e. its high accuracy might be due to the combination of poor sensitivity to change (in the method used) combined with a target that experienced little change.

- *Principal Components Analysis*. While this change detection method was not particularly difficult to execute, it required extra steps in the process that the other methods did not need. When we began the change detection research, the intuitive attraction to PCA was the fact that many bands could be used together -- no band selection was required. This was appealing because having more data in the process would suggest a greater ability to detect change. However, when applied to the Las Vegas study area, PCA demonstrated a poor ability to accurately identify areas of change/no change. As mentioned in the literature review, the results of PCA as a change detection method have been mixed. Las Vegas is apparently one of those areas where its performance is poor.

To a certain extent, some of the results of this research are counterintuitive. For example, common wisdom found in the literature suggests that image ratioing should produce much higher accuracies than image differencing. This is because image ratioing removes the effect of atmospheric differences between the two dates. However, in our test area, image subtraction was only slightly inferior to image ratioing.

In addition, as mentioned above, PCA should have been an overall superior method because 1) more variables (i.e. bands) could be included in the change detection process, 2) atmospheric effects are removed as a source of variability, and 3) it is a statistical method known to effectively summarize a set of correlated variables into a sequence of new variables in order of descending variance. Given that landscape change produces variance in landscape reflectivity, PCA would seem to be an excellent fit for change detection analysis. Nonetheless, as mentioned above, it was a poor contender in the Las Vegas study area.

The last counterintuitive result was the general observation that the green band was slightly superior for detecting change than the other two bands; i.e. in most cases, analyzing the green band produced higher change detection accuracy than either the red or near infrared band. Textbook wisdom states that the red and near-infrared bands are almost always the “safe bet” bands to use for a change detection application.

The apparent disagreement between the Las Vegas results and conventional wisdom confirms the maxim that remote sensing targets are all unique, and a measure of experimentation will always be necessary to find optimal approaches.

#### (4.2) Objective 3: Threshold Specification

When this research began, the threshold specification issue loomed large over the entire work. It was a necessary complication of each approach tested. As mentioned many times, the fear of the threshold issue was due to the fact that it created a point of decision that was subjective and greatly impacted the accuracy of the change prediction maps. In research, an objective approach to decision-making that relies on a metric of goodness (that can be optimized) is always preferred to a subjective approach. In addition, a subjective matter that has little impact on the final results is not a point of worry for most researchers. The choice of threshold in change detection is the worst possible research scenario, for it is *both* subjective *and* high impact. However, the result of our simple repetitive procedure to objectively calibrate the threshold value using a separate calibration field data set completely eliminated threshold specification as an issue. To our knowledge, this simple calibration approach has not been used by change detection researchers to-date. In this study, this calibration was done by automatically executing the change detection algorithms using 100 different threshold values within a

reasonable range and choosing the one that produced the highest accuracy with the calibration data. The complication that this approach presents to future research is that two sets of ground truth data must be gathered. The first set would be used for *calibration* of the change detection methods, i.e. determining the optimal threshold value. The second set would be used for *validation*, i.e. determining the actual accuracy of the change detection algorithm. To make this iterative approach work, it is essential that the practitioner plan on having a design and budget which permits the collection of two distinct ground truth data sets of sufficient size.

#### (4.3) Summary

This research constituted a study of methodology, not a study of urban change itself. It examined several change detection algorithms yielding change/no-change results. In Table 1, as outlined in Chapter 2, the advantages and disadvantages of each method applied in this research is described with its corresponding literature. In Table 2 we presented the accuracy results from the change detection method. Each of the methods accurately identified areas of change/no change with moderate levels of accuracy.

After a thorough execution of each change detection method and its subsequent threshold selection, it is clear that the determination of thresholds for each technique is critical to its success. Moreover, the type of statistic used in optimizing the change cutoff is significant. In other words, the measure used to describe the "goodness" of a change map has significant implications when selecting a cutoff threshold between change and no change. The approach of using a calibration and validation ground truth data set has significant merit.

The examination of these methods adds to the body of knowledge by providing a measure of guidance for future researchers and analysts performing change detection methods over similar targets. Additionally, utilizing urban change detection in an arid environment and its methodologies provides a detailed “jumping off” point for urban planners and policy makers to make informed decisions that may impact natural resources, surrounding environments and natural ecosystems, urban quality of life, and infrastructure needs.

Beyond these vital applications of change detection methodology domestically is the impact that such research could have for military strategies and political approaches abroad. Since 9/11 the United States has engaged in the War on Terrorism that has taken this country’s war fighters to two separate fronts: the Afghanistan/Pakistan border and Iraq. More recently, the Arab Spring has caused a US presence in Libya with potential for boots on the ground in Syria and Yemen. The Arab Spring has also caused disruption to many of America’s allies: Egypt, Algeria, and Qatar. The study of change detection methodologies in this thesis is unique in that the results focus on a study area in the desert regions of the greater Las Vegas area. Similarly, the various fronts engaged in by the United States as well as those of our allies possess similar physical geographies sensitive to terrorist operations, training, and planning as well as state governments and civic protesters attuned to their movements. The application of the change detection methods used in this thesis are beneficial to those studying the activities, development, and patterns of terrorists and other independent entities in regions with similar geography and may provide solutions and a course of action for future applications to support the war fighter and intelligence community alike.

Table 1. Summary of Statistics by Change Detection Technique

Algorithm	Band	Threshold	Accuracy	Minimum Chi-Square
<b>Category I. Algebra</b>				
Image Difference	Green	0.0488	74.80%	0.0452
	Red	0.0685	74.20%	0.1016
	NIR	0.0697	74.80%	0.1807
Image Ratio	Green	0.102	75%	0.102
	Red	0.13	75.60%	0.045
	NIR	0.114	74.80%	0.045
Image Regression	Green	0.0215	67.20%	0.045
	Red	0.0301	66.40%	0.045
	NIR	0.0327	66%	0.181
Vegetation Index Differencing	Red/NIR	0.052	65%	0.052
<b>Category II. Transformation</b>				
Principal Components Analysis	Green/Red/NIR Component 1	0.176	64.80%	0.0452
	Green/Red/NIR Component 2	0.07	74.60%	0.1016
	Green/Red/NIR Component 3	0.0441	61.80%	0.9147
	Green/Red/NIR Component 4	0.0149	65%	1.3665
	Green/Red/NIR Component 5	0.0126	60%	0.7228
	Green/Red/NIR Component 6	0.0045	70.20%	0.0113

## References

- Almutairi A., and T. A. Warner, "Change Detection Accuracy and Image Properties: A Study Using Simulated Data," *Remote Sensing* 2, no.6 (2010): 1508-1529.
- ASPRS Annual Conference 2006, "Mapping Urban Land Cover Using Quickbird NDVI Image and GIS Spatial Modeling for Runoff Coefficient Determination," Pravara Thanapura, Dennis Helder, Suzette Burckhard, Eric Warmath, Mary O'Neill, and Dwight Galster.  
<http://www.asprs.org/a/publications/proceedings/reno2006/0153.pdf> (accessed 27 November 2012)
- Asian Conference of Remote Sensing 2000: Poster Session 1, "Applications of Hyperspectral Remote Sensing in Urban Regions," Suni Bhaskaran and Bisun Datt. <http://www.gisdevelopment.net/aars/acrs/2000/ps1/ps112pf.htm> (accessed May 9, 2006).
- Asian Conference of Remote Sensing 1997: Land Use, "Operational Urban Sprawl Monitoring using Satellite Remote Sensing: Excerpts from the Studies of Ahmedabad, Vadodara and Surat, India," P. Jothimani.  
<http://www.gisdevelopment.net/aars/acrs/1997/ts8/ts8005pf.htm> (accessed May 9, 2006).
- Berberoglu, S. and A. Akin, "Assessing Different Techniques to Detect Land Use/Cover Changes in the Eastern Mediterranean," *International Journal of Applied Earth Observation and Geoinformation*, no.11 (2009): 46-53.
- Burchell, R. W., Downs, A., McCann, B. and S. Mukherji. *Sprawl Costs: Economic Impacts of Unchecked Development*. Washington, DC: Island Press, 2005.
- Byrne, G., Crapper, P. and K. Mayo, "Monitoring Land-Cover Change by Principal Components Analysis of Multitemporal Landsat Data," *Remote Sensing of Environment*, no.10 (1980): 175-184.
- Ceballos, J.C., and M.J. Bottino, "The Discrimination of Scenes by Principal Components Analysis of Multi-Spectral Imagery," *International Journal of Remote Sensing*, no.18 (1997): 2437-2449.
- Chander, G., Markham, B., and D. Helder, "Summary of Current Radiometric Calibration Coefficients for Landsat MSS, TM, ETM+, and EO-1 ALI Sensors," *Remote Sensing of the Environment*, no.113 (2007): 893-903.
- City of Las Vegas: Las Vegas, Nevada. [www.lasvegasnevada.gov](http://www.lasvegasnevada.gov) (accessed 27 November 2012).

- Clarke, Keith C. *Exploring the Urban Community: A GIS Approach*. Upper Saddle River, New Jersey: Pearson Prentice Hall, 2006.
- Coppin, P.R. and M.E. Bauer, M.E. 1996. Digital Change Detection in Forest Ecosystems with Remote Sensing Imagery. *Remote Sensing Reviews* 13, no.3 (1996): 207-234.
- Davis, C. and T. Schaub, "A Transboundary Study of Urban Sprawl in the Pacific Coast Region of North America: The Benefits of Multiple Measurement Methods," *International Journal of Applied Earth Observation and Geoinformation*, no.7 (2005): 268-283.
- Earth Observatory: Salt Lake City, Utah. Julie A. Robinson. [http://earthobservatory.nasa.gov/Newsroom/NewImages/images.php3?img\\_id=15361](http://earthobservatory.nasa.gov/Newsroom/NewImages/images.php3?img_id=15361) (accessed June 8, 2006).
- Epstein, J., K. Payne, and E. Kramer, "Techniques for Mapping Suburban Sprawl," *Photogrammetric Engineering and Remote Sensing* 63, no.9 (2002): 913-918.
- Glaeser, E.L. and M.E. Kahn, "Sprawl and Urban Growth," *NBER (National Bureau of Economic Research, Inc.) Working Paper Series*, no. 9733 (2003): 1-44.
- Herold, M., Goldstein, N.C., and K.C. Clarke, "The Spatiotemporal Form of Urban Growth: Measurement, Analysis and Modeling. *Remote Sensing of the Environment*, no.86 (2003): 286–302.
- Howell-Moroney, M., "Studying the Effects of the Intensity of US State Growth Management Approaches on Land Development Outcomes," *Urban Studies* 44, no.11 (2007): 2163-2178.
- Imhoff, M.L., E. Levine, M.V. Privalsky, V. Brown, W.T. Lawrence, C.D. Elvidge, and T. Paul, "Using Nighttime DMSP/OLS Images of City Lights to Estimate the Impact of Urban Land Use on Soil Resources in the United States," *Remote Sensing of Environment* 59, no.1 (1997): 105-117.
- International Conference on Applied Life Sciences 2012: "Monitoring Land Use/Cover Changes Using Different Change Detection Techniques (Case Study: Falavarjan Area, Isfahan, Iran)," Maliheh Alsadat Madanian, Alireza Soffianian, and Sima Fakheran. [http://cdn.intechopen.com/pdfs/39888/InTech-Monitoring\\_land\\_use\\_cover\\_changes\\_using\\_different\\_change\\_detection\\_techniques\\_case\\_study\\_falavarjan\\_area\\_isfahan\\_iran .pdf](http://cdn.intechopen.com/pdfs/39888/InTech-Monitoring_land_use_cover_changes_using_different_change_detection_techniques_case_study_falavarjan_area_isfahan_iran.pdf) (accessed 26 November 2012).

Jabbar, M.T. and X. Zhou, "Eco-environmental Change Detection by Using Remote Sensing and GIS Techniques: A Case Study Basrah Province, South Part of Iraq." *Environmental Earth Sciences*. (2011).

Jensen, J.R. *Introductory Digital Image Processing: A Remote Sensing Perspective*. Upper Saddle River, New Jersey: Pearson Prentice Hall, 2005.

Jensen, J.R., "Urban Change Detection Mapping Using Landsat Digital data," *The American Cartographer*, no.8 (1981): 127-147.

Klemas, V., "Remote Sensing of Wetlands: Case Studies Comparing Practical Techniques," *Journal of Coastal Research* 27, no.3 (2011): 418-427.

Ki-moon, Ban. 2008. UN-HABITAT [www.unhabitat.org](http://www.unhabitat.org) (accessed 25 November 2012).

Land Cover Classification. 2012. NASA Earth Observatory. Greenbelt, MD: Author. [http://earthobservatory.nasa.gov/Features/LandCover/land\\_cover.php](http://earthobservatory.nasa.gov/Features/LandCover/land_cover.php) (accessed 22 November 2012).

Levien, L.M., C.S. Fischer, P.D. Roffers, and B.A. Maurizi, "Statewide Change Detection Using Multitemporal Remote Sensing Data," Presented at the First International Conference on Geospatial Information in Agriculture and Forestry, Lake Buena Vista, Florida, 1-3 June 1998.

Li, X. and M. Damien, "Coastline Change Detection with Satellite Remote Sensing for Environmental Management of the Pearl River Estuary, China," *Journal of Marine Systems*, no.82 (2010): S54-S61.

Liu, Y., S. Nishiyama, and T. Yano, "Analysis of Four Change Detection Algorithms in Bi-temporal Space with a Case Study," *International Journal of Remote Sensing* 25, no.11 (2004): 2121-2139.

Lu, D., P. Mausel, E. Brondizio, and E. Moran, "Change Detection Techniques," *International Journal of Remote Sensing*, no. 25 (2004): 2365-2407.

Lunetta, R., J. Knight, J. Ediriwickrema, J. Lyon, and L. Worthy, "Land- cover Change Detection Using Multi-temporal MODIS NDVI Data," *Remote Sensing of Environment*, no.105 (2006): 142-154.

Macleod, R.D., and R.G. Congalton, "A Quantitative Comparison of Change Detection Algorithms for Monitoring Eelgrass from Remotely Sensed Data," *Photogrammetric Engineering & Remote Sensing* 64, no.3 (1998): 207-216.

Mas, J.F., "Monitoring Land-cover Changes: A Comparison of Change Detection Techniques," *International Journal of Remote Sensing*, no. 20 (1999): 139-152.

- Masek, J.G., F.E. Lindsay, and S.N. Goward, "Dynamics of Urban Growth in the Washington DC Metropolitan Area, 1973-1996, from Landsat Observations," *International Journal of Remote Sensing*, no.21 (2000): 3473-86.
- Nelson, R.F., "Detecting Forest Canopy Change Due to Insect Activity Using Landsat MSS," *Photogrammetric Engineering & Remote Sensing*, no.49 (1983): 1303-1314.
- Prakash, A., and R.P. Gupta, "Land-use Mapping and Change Detection in a Coalmining Area - A Case Study in the Jharia Coalfield, India," *International Journal of Remote Sensing*, no.19 (1998): 391-410.
- Quarmby, N.A. and J.L. Cushnie, "Monitoring Urban Land Cover Changes at the Urban Fringe from SPOT HRV Imagery in South-east England," *International Journal of Remote Sensing* 10, no.6 (1989): 953-963.
- Rahdary, V., A. Soffianian, S. Maleki Naifabdai, S.J. Khajeddin, and Pahlavanravi, "Land Use and Land Cover Change Detection of Mouteh Wildlife Refuge Using Remotely Sensed Data and Geographic Information System," *World Applied Sciences Journal* 3, no.1 (2008): 113-118.
- Ridd, M. K., and J.D. Hipple, "Remote Sensing of Human Settlements," *Manual of Remote Sensing* 5, no.5 (2006).
- Ridd, M.K. and J. Liu, "A Comparison of Four Algorithms for Change Detection in an Urban Environment," *Remote Sensing of Environment*, no.63 (1998): 95-100.
- Robinson, J.W., "A Critical Review of the Change Detection and Urban Classification Literature," Technical memorandum CSCjTM-7916235, Computer Sciences Corporation, Silver Springs, Maryland, USA (1979).
- Rouse, J.W., R.H. Haas, D.W. Deering, and J.A. Schell, "Monitoring the Vernal Advancement and Retrogradation (Green Wave Effect) of Natural Vegetation," Final Rep RSC 1978-4, Remote Sensing Center, Texas A&M University, College Station, (1974).
- Singh, A., "Digital Change Detection Techniques Using Remotely Sensed Data," *International Journal of Remote Sensing*, no.10 (1989): 989-1003.
- Squires, G.D. *Urban Sprawl: Causes, Consequences & Policy Responses*. The Urban Institute Press, 2002.
- Squires, G.D. and C.E. Kubrin, "Privileged Places: Race, Uneven Development and the Geography of Opportunity in Urban America," *Urban Studies* 42, no.1 (2005): 47-68.

- Srvastava, V.K., "Application of Remote Sensing and GIS Techniques in Monitoring of Urban Sprawl in and Around Jharia Coalfields (Dhanbad)," *Urban Planning Applications*, (1980).
- Stow, D.A., D. Collins, and D. McKinsey, "Land Use Change Detection Based on Multi-date Imagery from Different Satellite Sensor Systems," *Geocarto International*, no.5 (1990): 3–12.
- Sunar, F., "An Analysis of Changes in a Multi-date Data Set: A Case Study in the Ikitelli Area, Istanbul, Turkey," *International Journal of Remote Sensing* 19, no.2 (1998): 225–235.
- Theau, J., "Change Detection," in *Encyclopedia of GIS*, ed. Shashi Shekhar and Hui Xiong (New York: Springer, 2008), 77-84.
- Toll, D.L., A. Royali, and J.B. Davis, "Urban Area Update Procedures Using Landsat Data," *Proceedings of the Fall Technical Meeting of the American Society of Photogrammetry held in Niagra Falls, Canada, in 1980* (Falls Church, Virginia: American Society of Photogrammetry), (1980): RS-EI-17.
- Townsend, P.A., C.O. Justice, C. Gurney, and J. McManus, "The Impact of Misregistration on Change Detection," *IEEE Transaction on Geoscience and Remote Sensing* 30, no.5 (1992): 1054-1060.
- United States Census 2010. 2010. U.S. Census Bureau.  
<http://2010.census.gov/2010census/data/> (accessed 27 November 2012).
- Vermont Forum on Sprawl. 2003. *What is Sprawl?* Burlington, VT: Author.  
<http://www.vtsprawl.org> (accessed May 5, 2006).
- Xian, G., M. Crane, and C. McMahon, "Quantifying Multi-temporal Urban Development Characteristics in Las Vegas from Landsat and ASTER Data," *Photogrammetric Engineering & Remote Sensing* 74, no.4 (2008): 473-481.
- Xiao, J., S. Yanjun, G. Jingfeng, T. Ryutaro, T. Changyuan, L. Yangting, and H. Zhiying, "Evaluating Urban Expansion and Land Use Change in Shijiazhuang, China, by Using GIS and Remote Sensing," *Landscape and Urban Planning*, no.75 (2006): 69-80.
- Yang, L., X. George, J. Klaver, and B. Deal, "Urban land cover Change Detection Through Sub-pixel Imperviousness Mapping Using Remotely Sensed Data," U.S. Geological Survey Contract 1434-CR-97-CN-40274, (2003).  
[http://scholar.google.com/scholar?hl=en&lr=&client=firefox-a&q=cache:3YsWPUF24wgJ:dodesp.er.usgs.gov/reports/urbanaspr\\_2003.pdf+author:%22Yang%22+intitle:%22Urban+land+cover+change+detection+through+sub-pixel+...%22+](http://scholar.google.com/scholar?hl=en&lr=&client=firefox-a&q=cache:3YsWPUF24wgJ:dodesp.er.usgs.gov/reports/urbanaspr_2003.pdf+author:%22Yang%22+intitle:%22Urban+land+cover+change+detection+through+sub-pixel+...%22+) (accessed May 8, 2006).

- Yeh, A. and X. Li, “An Integrated Remote Sensing and GIS Approach in the Monitoring and Evaluation of Rapid Urban Growth for Sustainable Development in the Pearl River Delta,” *International Planning Studies* 2, no.2 (1997): 193-210.
- Yu, X. and C. Ng, “An Integrated Evaluation of Landscape Change Using Remote Sensing and Landscape Metrics: A Case Study of Panyu, Guangzhou,” *International Journal of Remote Sensing* 27, no.6 (2006): 1075–1092
- Yuan, F. and M. Bauer, “Comparison of Impervious Surface Area and Normalized Difference Vegetation as Indicators of Surface Urban Heat Island Effects in Landsat Imagery,” *Remote Sensing of Environment*, (2006).